Scientific Research Publishing

American Journal of Plant Sciences, 2022, 13, 623-649
https://www.scirp.org/journal/ajps
ISSN Online: 2158-2750
ISSN Print: 2158-2742

Identification and Analysis of miRNAs and siRNAs in *Botrytis cinerea*

Yaoyao Liu*, Miao Sun*, Qinru Yu, Ran Li, Xu Hu, Pengcheng Zhang, Tongfei Lai, Ting Zhou#

College of Life and Environmental Science, Hangzhou Normal University, Hangzhou, China
Email: #zt20100061@163.com

How to cite this paper: Liu, Y.Y., Sun, M., Yu, Q.R., Li, R., Hu, X., Zhang, P.C., Lai, T.F. and Zhou, T. (2022) Identification and Analysis of miRNAs and siRNAs in *Botrytis cinerea*. *American Journal of Plant Sciences*, **13**, 623-649.
https://doi.org/10.4236/ajps.2022.135042

Received: March 31, 2022
Accepted: May 24, 2022
Published: May 27, 2022

Abstract

Small RNAs in *Botrytis cinerea* were analyzed via high-throughput sequencing on BGISEQ-500 platform. A total of 8 novel miRNAs and 110 novel siRNAs were predicted. Sequence information, construction, length distribution, base bias and expression levels of miRNAs and siRNAs were determined as well. Through GO and KEGG enrichment analysis, the miRNA target genes are mostly located in membrane and organelle, possessed binding and catalytic activities, and involved in signal transduction and carbohydrate metabolism. The results will provide a theoretical foundation for understanding the developmental and pathogenic mechanisms of *B. cinerea* at the transcriptional level.

Keywords

Botrytis cinerea, MicroRNA, Small Interfering RNA, Biological Function

1. Introduction

Botrytis cinerea is a necrotrophic plant pathogen with a broad host range, which can cause gray mold disease on crops, fruits and vegetables. This notorious fungus infects nearly all tissues of hosts at both pre-harvest and post-harvest stages, and leads to a huge economic loss worldwide. Owing to the importance in agricultural production, it has been ranked as the second most important plant-pathogenic fungus, and becomes one of the most extensively investigated pathogens [1]. Controlling this pathogen is difficult because of its various attack modes, great reproductive output, high evolutionary potential, and ability to survive for extended periods as conidia and/or small hardened mycelia masses called sclerotia. The application of synthetic fungicide is a conventional but not

*Yaoyao Liu and Miao Sun contributed equally to this work.
#Corresponding author.

an adequate strategy due to developed resistant strains and adverse effects on the environment and human health [2] [3]. Therefore, exploring the pathogenic mechanisms o*f B. cinerea* will provide a fundamental basis for developing new effective and safe control strategies. So far, a gapless genome sequence for *B. cinerea* strain B05.10 has been reported [4], and many advances have been achieved on the developmental and pathogenetic processes of *B. cinerea*, specifically on functional roles of genes in growth, virulence, metabolism, signaling and stress response [5] [6] [7]. These findings indicate the multigenic, variable, and sophisticated nature of necrotrophic pathogenicity of *B. cinerea*. Exploring more specific regulatory networks is necessary.

RNA has received extensive attention and it has been one of the most popular areas of life science research for nearly a decade. Non-coding RNA (ncRNA) does not encode a protein and performes the biological functions at the RNA level, such as ribosomal RNA (rRNA), transfer RNA (tRNA), microRNA (miRNA), small nuclear RNA, small interfering RNA (siRNA) and long non-coding RNA (lncRNA) [8] [9]. Among them, miRNAs are small non-coding RNAs of about 20 - 24 nucleotides, which can inhibit the translation of proteins by binding to 3'-UTR of the target mRNA [10]. Some studies found that miRNAs could interact directly with proteins to regulate gene expression or influence epigenetic mechanisms. Another, siRNAs are double-stranded RNAs of 20 - 25 nt. A guide strand of siRNA is selected and incorporated into the RNA-induced silencing complex (RISC). The siRNA guides RISC to fully complementary sites on target RNA that is then sequence-specifically cleaved by the Argonaute (Ago) protein. This process is named as RNA interference (RNAi) which leads to transcriptional or post-transcriptional gene silencing [11]. Although miRNA and siRNA share many similarities, both are short duplex RNA molecules that exert gene silencing effects by targeting mRNA, yet their mechanisms of action are distinct. The major difference between siRNA and miRNA is that the former is highly specific with only one mRNA target, whereas the latter has multiple targets. Many evidences have indicated that miRNA and siRNA could participate in gene expression, chromosome structure modification, cell differentiation, epigenetic regulation, and human disease. However, the identification and biological function analysis of miRNA and siRNA in fungal pathogens are less reported. In this study, small RNAs in *B. cinerea* were sequenced via high-throughput transcriptomic technology. The detected miRNAs and siRNAs were characterized and target genes of miRNAs were predicted. The results will provide a theoretical foundation for understanding pathogenic genes and regulatory pathways of *B. cinerea* at the transcriptional level.

2. Materials and Methods

2.1. Fungal Physiological Measurement

Botrytis cinerea was isolated from a naturally infected tomato fruit with a typical grey mold symptom. The genetic background of fungus has been identified by

morphological observation and rDNA-internal transcribed spacer analysis in the preliminary experiments. The fungus was cultivated on a potato dextrose agar (PDA) plate at 25˚C. To evaluate the mycelial growth, a mycelial agar disk (0.5 cm in diameter) was placed in the center of a 9 cm diameter petri dish containing 25 mL PDA. During 10 days of culturing at 25˚C, radial growth was measured daily by the decussation method. Meanwhile, the mycelial phenotype was microscopically observed using a Nikon Eclipse Ni-U microscope (Nikon, Japan). Tomato fruit at commercial maturity were bought from local market. After disinfection by 2% sodium hypochlorite, fruit were wounded at the equator utilizing a sterile needle and inoculated with 10 μL spore suspension (1×10^4 spores/mL). The lesion diameter of inoculated fruit was recorded in every two days.

2.2. Small RNA Sequencing

Fresh spore suspensions were prepared by flooding the sporulating cultures of *B. cinerea* with sterile distilled water containing 0.05% (v/v) Tween-20. A suitable aliquot of the suspension was added to 100 mL potato dextrose broth (PDB) with a final concentration of 1×10^6 spores/mL. After 24 h of shaking culture at 25˚C, the harvest spores and mycelia were washed twice with sterile distilled water, and quickly frozen in liquid nitrogen. A biological repeat was carried out, and the two samples were mixed with the same weight. Small RNA sequencing was performed using BGISEQ-500 technology of Beijing Genomics Institute (BGI) Co., Ltd. Briefly, small RNA was separated from total RNA by PAGE gel, and linked with a 5'-adenylated, 3'-blocked single-stranded DNA adapter at 3' end. After RT primer hybridization, the 5' adaptor was linked and the first strand cDNA was synthesized. To enrich cDNA of 100 - 120 bp, PCR amplification and PAGE gel separation were carried out. Finally, the library was quantified and pooling cyclization was performed. Each step was under strict quality control.

2.3. Bioinformatic Analysis

After sequencing, the original data were filtered by removing low-quality reads, adaptors and other contaminants to get clean reads. The remaining tags (clean tags or clean reads) were stored in FASTQ format. Bowtie2 was used to map clean reads to the reference genome and to other sRNA [12], and Cmsearch was used for Rfam [13]. sRNA classification followed the priority rule as MiRbase > pirnabank > snoRNA > Rfam > other sRNA. Novel miRNA was predicted by exploring the characteristic hairpin structure of miRNA precursor in miRDeep2 and miRA [14] [15]. siRNA predicting followed the criteria that siRNA was a 22 - 24 nt double-stranded RNA, each strand of which was 2 nt longer than the other [16]. The small RNA expression level was calculated by using TPM (transcripts per million). TPM = $C \times 10^4/N$. C means miRNA counts number in a sample, and N means total reads number that mapped to the genome [17]. TAPIR and

TargetFinder were used to predict miRNA target genes [18]. The default parameters are as follows, TAPIR: --score 5 --mfe_ratio 0.6; TargetFinder: -c 4. WEGO software was used to perform Gene Ontology (GO) enrichment analysis of miRNA target genes. KEGG database was used to perform pathway enrichment analysis of miRNA target genes. A scatter plot of the KEGG enrichment results and a bar plot of the KEGG terms were generated. A corrected P value ≤ 0.05 was taken as a threshold.

2.4. Statistical Analysis

Data were pooled across independent repeat experiments. Correlation analysis was carried out to test the significance of the relationship between two or more variables utilizing Statistical Product and Serviced Solutions software (SPSS, USA). Analysis of variance (ANOVA) was used to compare more than two means. Mean separations were analyzed using Duncan's multiple range test. Differences at $P < 0.05$ were considered to be significant.

3. Results

3.1. Phenotype and Activity of *B. cinerea*

In a previous experiment, the isolate has been identified as *Botrytis cinerea* based on morphological and genetic characteristcs. Typically, sclerotia of *B. cinerea* commence growth to produce conidiophores and multinucleate conidia, serving as a primary source of inoculum. Microconidia are also formed as spermatia. The sexual cycle involves the spermatization of sclerotia, leading to the production of apothecia and asci with eight binucleate ascospores. Conidia generation follows a cycle of initiation, production and dissemination that is controlled by changes in light, humidity and temperature. Dry-inoculated conidia produced one or two short germ tubes and no obvious terminal appressoria, whereas conidial within suspension possessed much longer germ tube and extensive secretion of an extracellular matrix. On PDA plate, *B. cinerea* initially formed white colony turning gray or grayish brown (**Figure 1(A)**). The mycelial extension was fast and the colony could cover the petri dish in 8 days (**Figure 1(C)**). The hyphae were septate and intertwined (**Figure 1(B)**). Conidiophores were gray brown, ellipsoidal or ovate.

B. cinerea is responsible for a very wide range of symptoms. Soft rots, accompanied by collapse and water-soaking of parenchyma tissues, followed by a rapid appearance of grey masses of conidia are the most typical symptoms on fruit. Soft rotting of mature tomato fruit occurs mainly in postharvest stage. In the present study, at the temperature of 25˚C with high relative humidity, the infection of *B. cinerea* ontomato fruit was rapid, resulting in softening of the flesh and a browning skin. On the fruit surface, massive mycelia were visible. Within about a week, the fruit was completely rotten (**Figure 1(D)**). Therefore, the fungus used in this study presented a typical phenotype of *B. cinerea*, and exhibited a normal growth and pathogenicity.

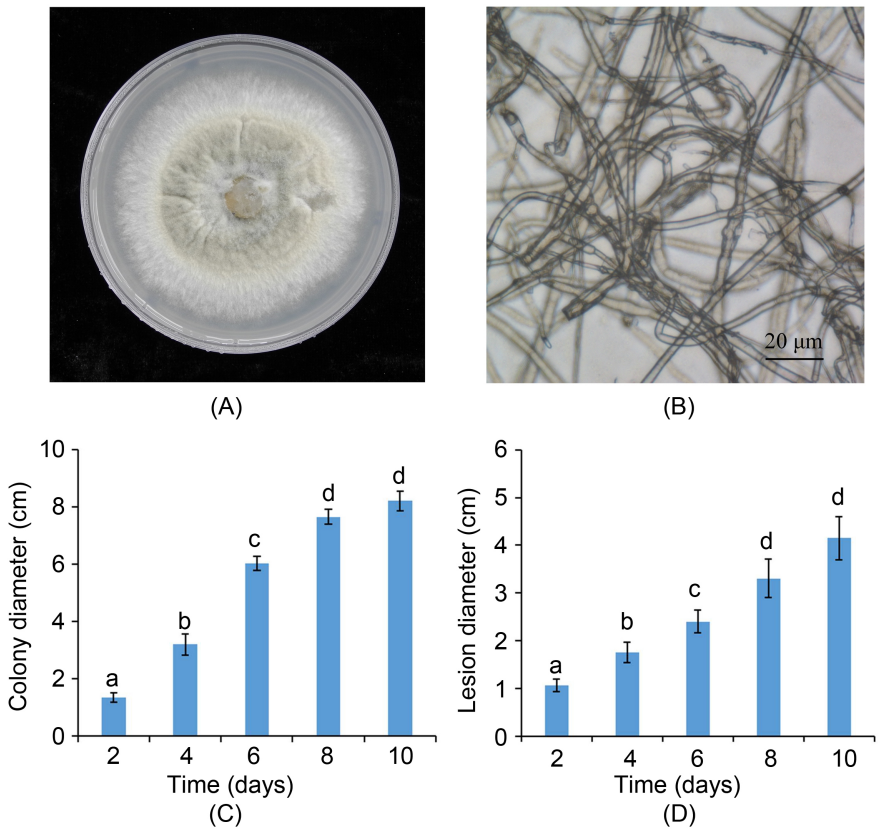

Figure 1. Phenotype and growth dynamic of *Botrytis cinerea.* (A) Colonial phenotype; (B) Mycelial phenotype; (C) Mycelial expansion on PDA; (D) Lesion expansion on tomato fruit. Bars represent the standard deviation of the means of three independent experiments. Lower case letters indicate significant differences at $P < 0.05$ at each time point.

3.2. Small RNA Sequencing Results

The small RNAs were sequenced using BGISEQ-500 technology. A total of 27,872,641 raw tags containing 1,006,245 low quality tags, 875,820 invalid adapter tags, 774 polyA tags, 1,934,729 short valid length tags and 24,055,073 clean tags. The base percentage composition of clean tags was shown in **Figure 2(A)**. The percentage of clean tags, of which quality was more than 20, was 98.80% of all clean tags (**Figure 2(B)**). The length of small RNAs was in a range of 10 - 44 nt, and the number of small RNAs in a range of 18 - 30 nt was the highest (**Figure 2(C)**). A total of 20,830,926 clean tags were aligned to the reference genome. Among them, 23,900 snRNAs, 1,187,863 rRNAs, 16,349 snoRNAs, 20,911 tRNAs, 270,355 Rfam other sncRNAs, and 10,932 precursors were identified. The proportion of all kinds of sRNA was shown in **Figure 3(A)** and the genome distribution of tags was shown in **Figure 3(B)**.

3.3. Prediction of miRNAs and siRNAs

Only miR-466i-5p as known miRNA was found in *B. cinerea.* It belonged to mmu-miR-466i-5p family and its hairpin contained 300 bases. Eight novel miRNAs named as Bc-mir1 to Bc-mir8 were predicted. Their expression levels

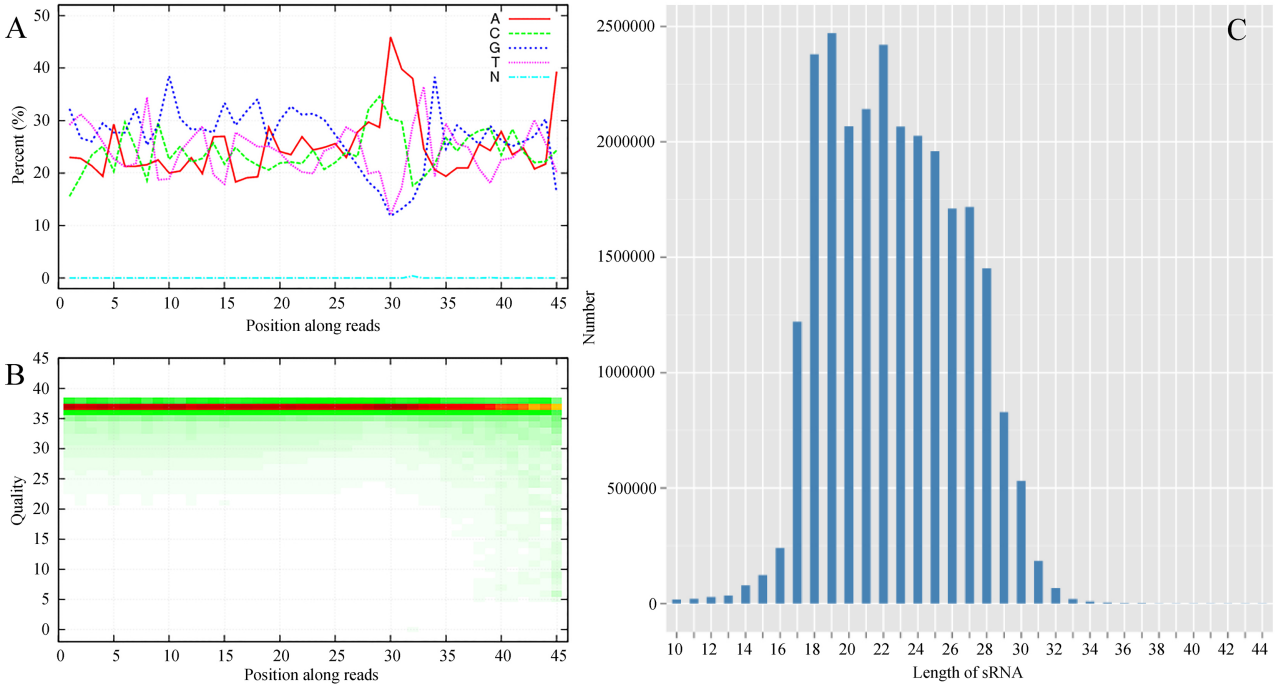

Figure 2. Sequencing results of small RNA in *B. cinerea*. (A) Base percentage composition of small RNAs; (B) Distribution of base quality on clean tag. Each dot represents the total number of bases with a specific quality value of the corresponding base along a tag, and a darker color indicates a higher base number; (C) Length distribution of small RNAs.

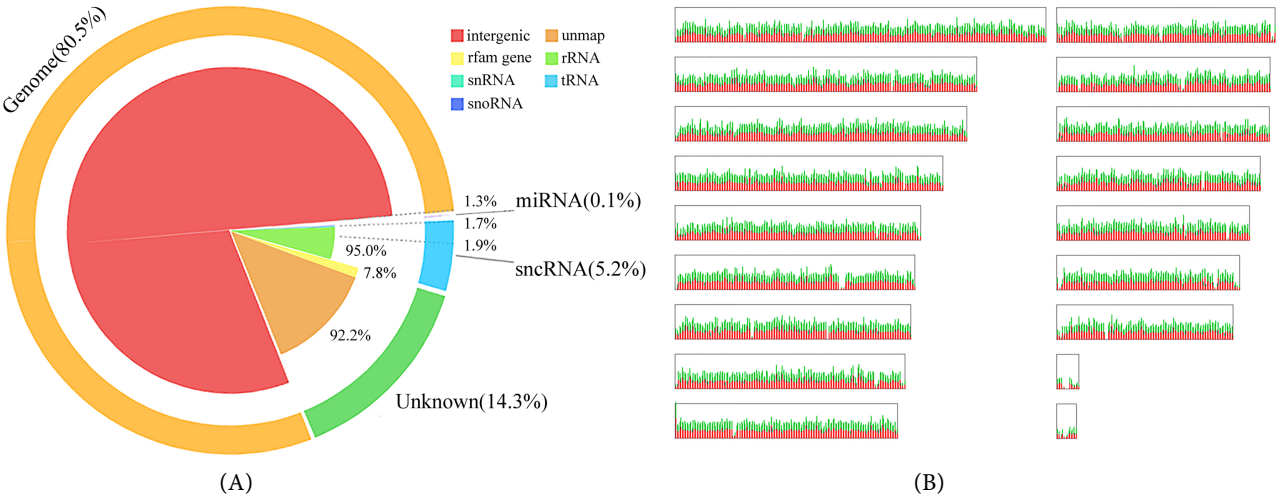

Figure 3. Catalog of small RNA (A) and genome distribution of tags (B). Figure (A) shows the proportion of different types of small RNA. In Figure (B), the X axis shows the relative position in the chromosome, and the Y axis shows the number of tags. The color red indicates tag count, whereas green indicates tag catalogs.

were significantly different. The expression of Bc-mir1 was about 100 times higher than that of Bc-mir8. The sequence information of novel miRNAs was shown in Table 1. The stem loop structure of precursors was shown in Figure 4. A total of 110 novel siRNAs were predicted based on their architectural features. The details of novel siRNAs were shown in Table S1. Their expression levels were represented by the TPM values in a range of 0 to 16.41. Through sequence analysis, the base

Table 1. Information of predicted miRNAs in *Botrytis cinerea*.

Name	Chromosome	Strand	Sequence (mature)	TPM
Bc-mir1	NC_037310.1	+	CCATACACAAGCTTCAGATCGGTGGA	28,306.92
Bc-mir2	NC_037314.1	+	AGTTCAGTGGTAGAATTCTTGCTTTGGG	2310.08
Bc-mir3	NC_037317.1	+	GTGGCTCAGTTGGTTAGAGCGTTGGTCTCA	2355.44
Bc-mir4	NC_037320.1	+	TTACTCTGCGGGCAATCTGGTTTTCGAA	680.29
Bc-mir5	NC_037323.1	+	GTGTTCGATTCACGGCAGTTGCA	2911.67
Bc-mir6	NC_037323.1	+	AGACTGAGGAGAATTGGGCATCCCGTCCGC	13,262.56
Bc-mir7	NC_037324.1	+	CTGCTACTATGATATATTGAATTTG	314.38
Bc-mir8	NC_037325.1	+	GACTGAAGAGAATTGGGCATCC	271.62

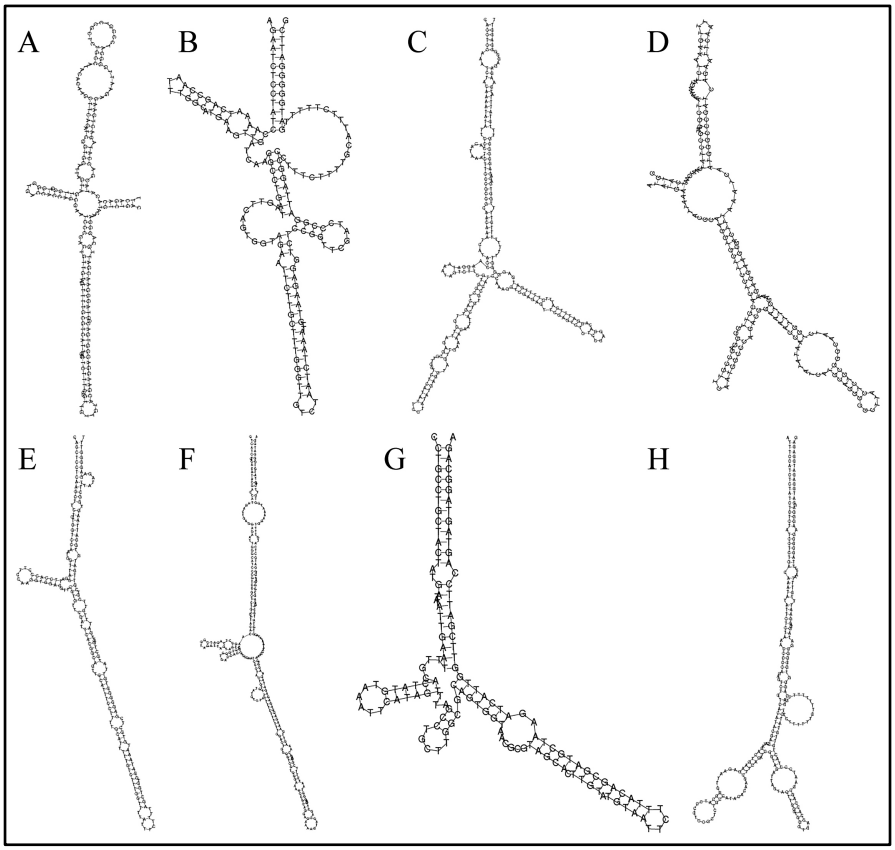

Figure 4. Stem-loop structure of predicted novel miRNA precursor in *B. cinerea*. (A)-(H) indicate the predicted miRNAs Bc-mir1 to Bc-mir8.

composition of predicted miRNAs and siRNAs was shown in Figure 5. For novel miRNAs, the first base distribution was G, C, A and U in number from high to low. There were no obvious rules for the base distribution due to the small number. The length of novel siRNAs was mostly less than 21 nt. The first base distribution was U, G, A and C in number from high to low. In the length range of 1 to 22 nt of all novel siRNAs, the third base contained the highest percent of G and lowest percent of U, and the twenty-second base possessed highest percent of U and lowest percent of

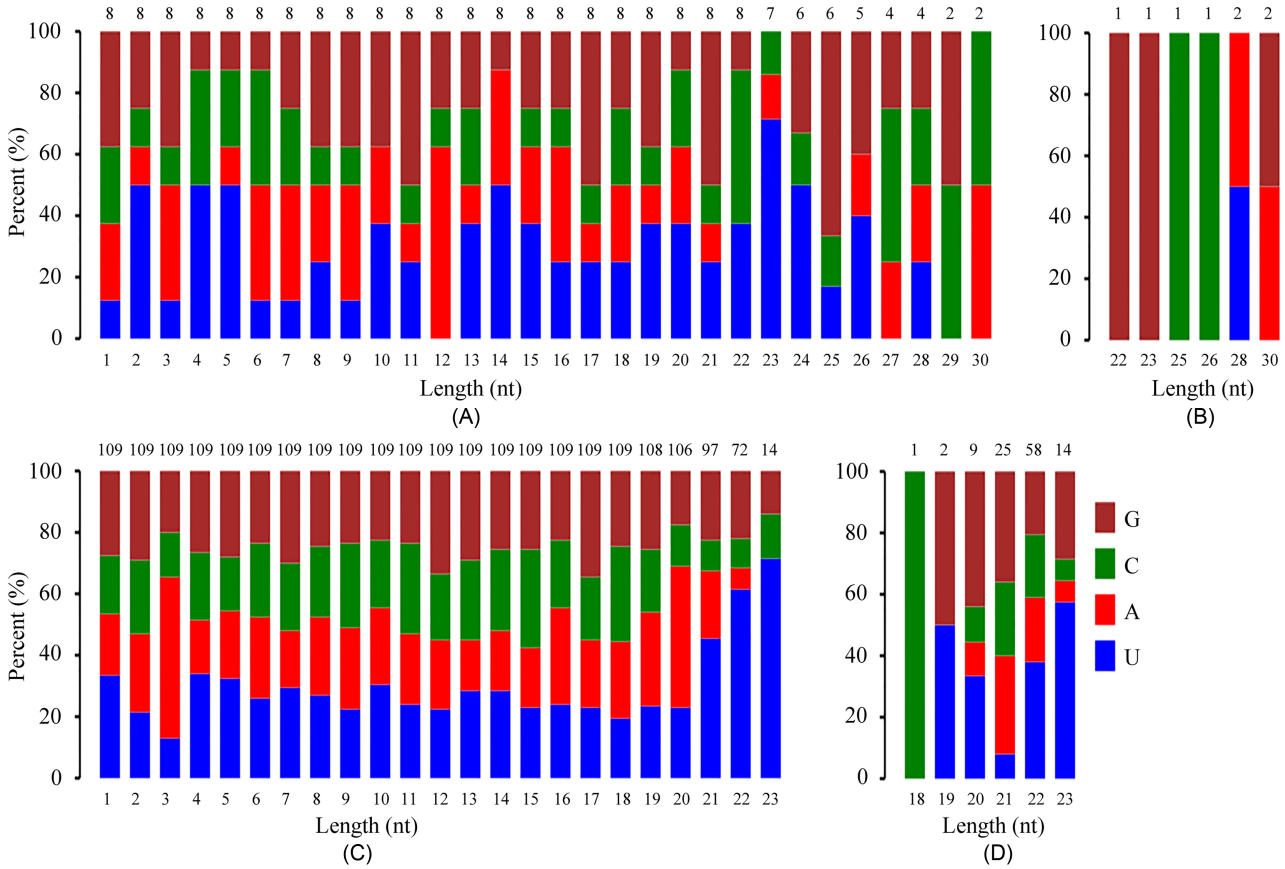

Figure 5. The base distribution in predicted miRNA and siRNA sequences in *B. cinerea*. (A) and (C) respectively indicate the base distribution in predicted miRNA and siRNA sequences; (B) and (D) respectively indicate the first base distribution of predicted miRNA and siRNA sequences.

A. In addition, the twenty-third base of 14 siRNAs did not contain base A.

3.4. Enrichment Analysis of miRNA Target Genes

Software TAPIR and TargetFinder were used to find the target genes of miRNAs in *B. cinerea*. The intersection results of two softwares contained 300 target genes, and there were 642 target genes in union results (**Table S2**). The GO enrichment result was shown in **Figure 6**. Most of the target genes located in membrane and organelle, and possessed binding activity, catalytic activity or transporter activity. The target genes involved in many biological processes including cellular process, biological regulation, metabolic process, single-organism process, etc. The KEGG enrichment result was shown in **Figure 7**. The items with a larger number of target genes were carbohydrate metabolism, signal transduction, and transport and catabolism. In addition, statistics of pathway enrichment indicated that many target genes were related to the MAPK signaling pathway, amino sugar and nucleotide sugar metabolism, and endocytosis. Meanwhile, target genes involved in the AGE-RAGE signaling pathway, alpha-linolenic acid metabolism, and phosphatidy linositol signaling system possessed higher rich factor value (**Figure 8**).

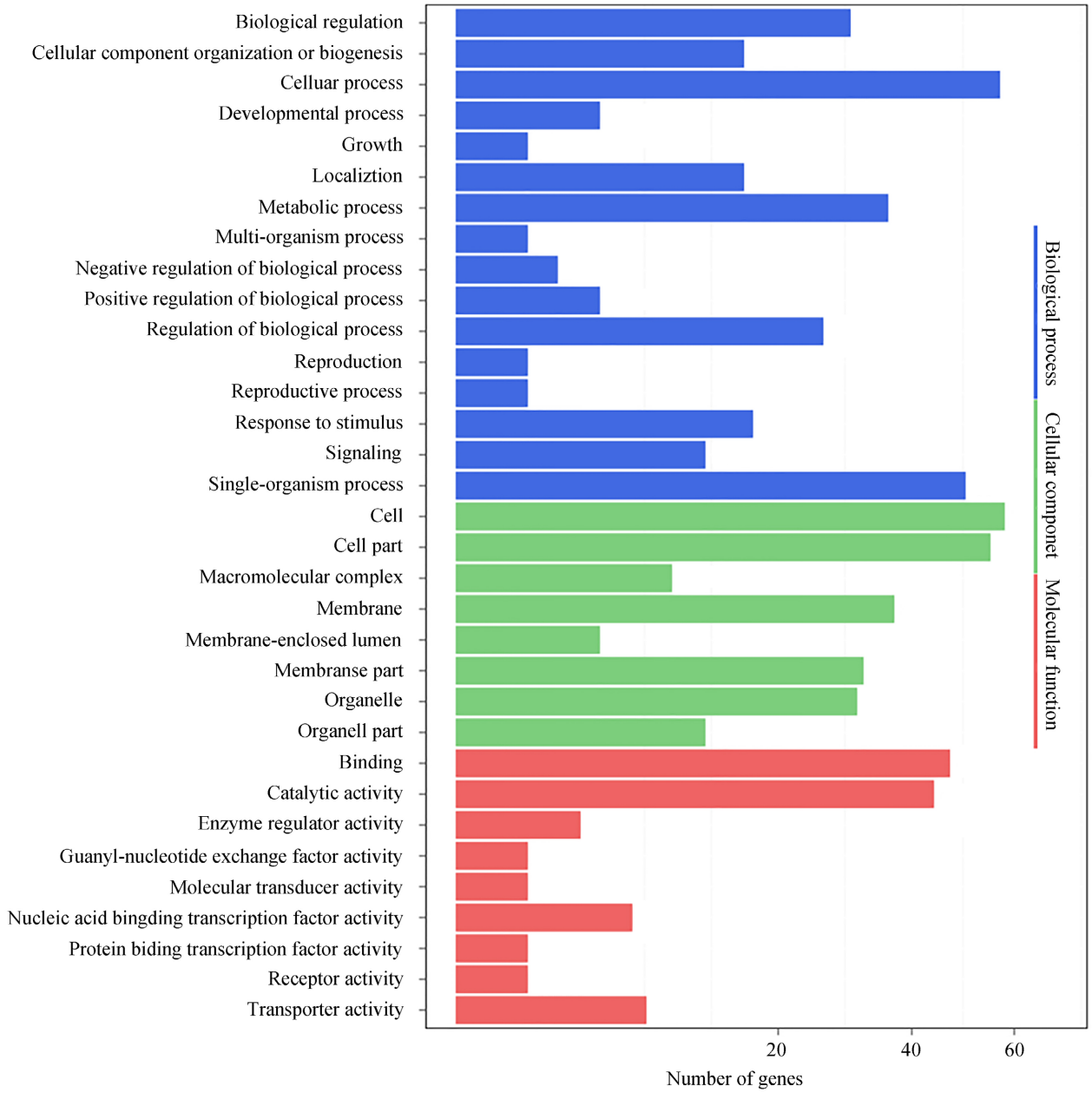

Figure 6. Gene Ontology (GO) functional classification of miRNA target genes in *B. cinerea*. The X axis means number of target genes. The Y axis represents GO term. All GO terms are grouped into three ontologies: blue is for biological process, green is for cellular component and red is for molecular function.

4. Discussion

RNAi is a highly conserved biological process in diverse species. It has in common the involvement of miRNAs and siRNAs. miRNAs are essential components of the gene silencing machinery in most eukaryotic organisms, and negatively regulate the expression of a large proportion of cellular mRNAs. Most of the miRNAs are transcribed by RNA polymerase II. The long primary transcript with a hairpin structure is termed as pri-miRNA. In the nucleus, pri-miRNA is converted into pre-miRNA (about 70 nt stem-loop precursor miRNA) under

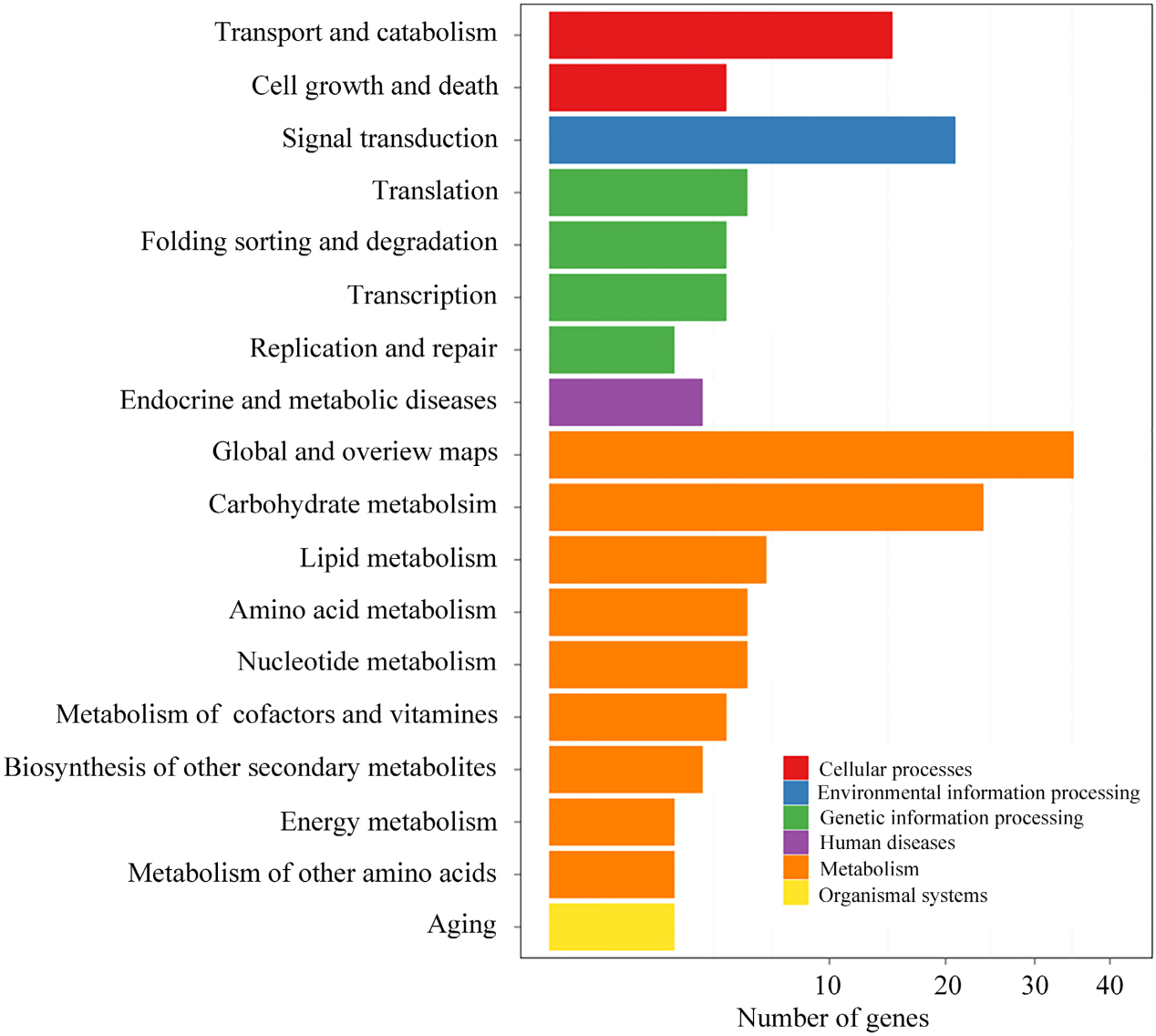

Figure 7. KEGG classification of miRNA target genes in *B. cinerea*. The X axis means number of target genes, The Y axis shows the second KEGG pathway terms and the first pathway terms are indicated using different colors.

catalyzing of RNase III type enzyme DROSHA and the double-stranded RNA-binding protein DGCR8. Once exported to the cytoplasm by Exportin-5, the pre-miRNA is processed to form miRNA duplex by another RNase type III enzyme Dicer. miRNA duplex is then incorporated in RISC together with Ago protein, where one strand is selected to become the mature miRNA [19]. The mature miRNA recognizes its complementary sequence in the 3' untranslated region of their target mRNAs via seed region, typically positions 2 - 7 in the miRNA. Then, miRNA exerts its regulatory functions through mRNA cleavage, deadenylation or translational repression [20] [21]. In addition, many studies have shown that a single miRNA may target multiple mRNAs, and some miRNAs with distinct sequences could repress the same target mRNA. For filamentous fungi, Lee *et al.* (2010) first found four different pathways for miRNAs

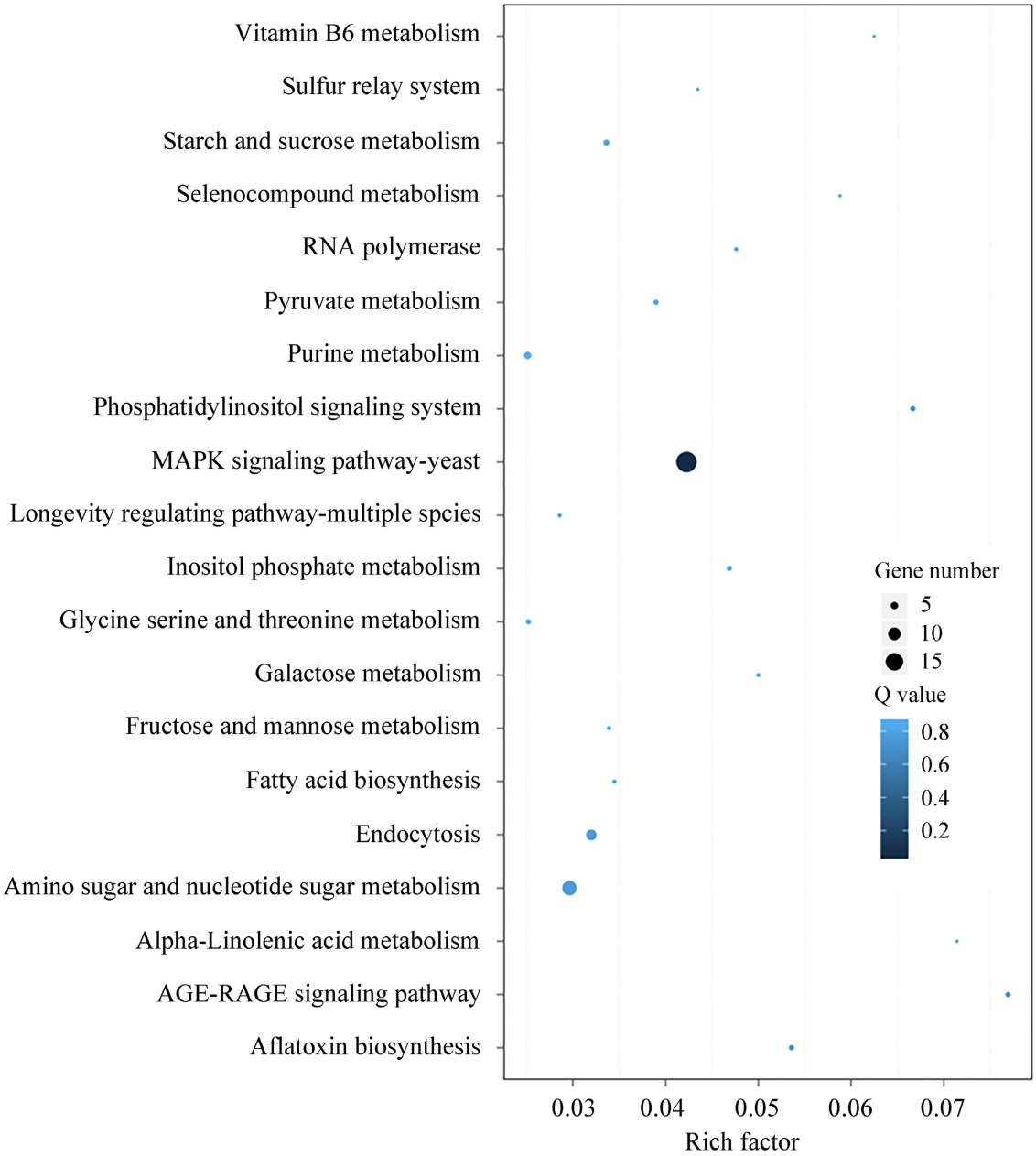

Figure 8. Statistics of pathway enrichment of miRNA target genes in *B. cinerea*. The rich factor is the ratio of target gene numbers annotated in this pathway term to all gene numbers annotated in this pathway term. The greater rich factor indicates the greater the degree of enrichment. The Q-value is the corrected *p*-value, and the lower Q-value indicates the greater enrichment level.

and siRNAs production in *Neurospora crassa*, which used a distinct combination of factors including Dicers, QDE-2, QIP, and MRPL3 [22]. Lin *et al.* (2015) identified 4 conserved miRNAs and 63 novel predicted miRNAs in *Antrodia cinnamomea*. Their predicted targets involved in triterpenoid synthesis, mating type recognition, chemical or physical sensory protein and transporters [23]. Wang *et al.* (2017) reported a novel miRNA (termed Pst-milR1) in *Puccinia striiformis* f. sp. tritici, which acted as an important pathogenicity factor sup-

pressing host immunity [24]. Jin *et al.* (2019) identified a novel milRNA VdmilR1 in *Verticillium dahlia* that could target *VdHy1* gene at the 3'-UTR for transcriptional repression through increased histone H3K9 methylation of *VdHy1* [25]. Hu *et al.* (2022) found an Ago1-associated miRNA (miR8788) that could target a potato alpha/beta hydrolase-type encoding gene (*StABH1*) and facilitate infection of *Phytophthora infestans* [26].

siRNA is processed from a long double-stranded RNA (dsRNA) which is commonly generated by RNA-dependent RNA polymerase (RdRP). Further, a RNase III-type Dicer ribonuclease cleaves dsRNA into siRNA with two unpaired nucleotides at the 3'-end of each strand. A guide strand is selected and associated with an Ago family protein to form RISC. The siRNA directs RISC to target homologous mRNA, which is then sequence-specifically cleaved by the Ago protein. This process finally leads to target gene silencing by RNA degradation, translational inhibition, or transcriptional silencing initiated by alteration of chromatin state [27] [28] [29]. In fungi, Khatri and Rajam (2007) found that a 23-nucleotide siRNA based on *ODC* (*ornithine decarboxylase*) gene could cause a specific silencing effect, and lead to significant reduction in mycelial growth and cellular polyamine concentration [30]. Hammond *et al.* (2013) identified and characterized two novel proteins, SAD-4 and SAD-5. Both of them were required for meiotic silencing by unpaired DNA and siRNA generation in *Neurospora crassa* [31]. Deshmukh and Purohit (2014) used synthetic siRNAs to down-regulate secondary metabolite genes *hmgR* and *fpps*, which led to bikaverin overproduction in *Fusarium* sp. HKF15 [32]. Yu *et al.* (2014) showed that convergent antisense transcription and availability of the Dicer ribonuclease were key determinants for heterochromatin formation and catalyzing siRNA generation in *Schizosaccharomyces pombe* [33]. Yu *et al.* (2021) found that trimethylguanosine synthase 1 (Tgs1) played critical roles in Swi6/HP1-independent siRNA production and establishment of heterochromatin in fission yeast [34].

Considering the critical roles of miRNAs and siRNAs in gene regulating and biological function in fungi, the specific and sensitive detection is becoming more important. More elaborate regulation mechanisms of miRNAs and siRNAs need to be further explored. Due to the short sequence lengths, large variability in per-cell copy number, and high sequence similarity within families, the relevant studies of miRNAs and siRNAs in *B. cinerea* are limited so far. Our study focuses on finding novel miRNAs and siRNAs, and the targets of miRNAs in *B. cinerea.* The results will provide new knowledge regarding the small RNA transcriptome and new insights into miRNAs function on pathogenicity and growth in *B. cinerea.*

5. Conclusion

In this study, 8 novel miRNAs and 110 novel siRNAs were predicted in *Botrytis cinerea* utilizing high-throughput transcriptomic sequencing. Their sequence information, construction, base bias and expression level were determined as

well. In addition, GO and KEGG enrichment analysis indicated that the miRNA target genes are mostly located in membrane and organelle, possessed binding and catalytic activities, and involved in carbohydrate metabolism and signal transduction. These results will provide new clues to understand the developmental and pathogenic mechanisms of *B. cinerea* at the transcriptional level.

Acknowledgements

This research was financially supported by the Zhejiang Provincial Natural Science Foundation of China (LY22C150009), Undergraduate Innovation Ability Improvement Project of Hangzhou Normal University (CX2021159) and Scientific Research Fund of Zhejiang Provincial Education Department (Y202044822).

Conflicts of Interest

The authors declare no conflicts of interest regarding the publication of this paper.

References

[1] Cheung, N., Tian, L., Liu, X.R. and Li, X. (2020) The Destructive Fungal Pathogen *Botrytis cinerea*—Insights from Genes Studied with Mutant Analysis. *Pathogens*, **9**, 923. https://doi.org/10.3390/pathogens9110923

[2] Leroux, P., Fritz, R., Debieu, D., Albertini, C., Lanen, C., Bach, J., Gredt, M. and Chapeland, F. (2002) Mechanisms of Resistance to Fungicides in Field Strains of *Botrytis cinerea. Pest Management Science*, **58**, 876-888. https://doi.org/10.1002/ps.566

[3] González-Domínguez, E., Fedele, G., Caffi, T., Delière L., Sauris, P., Gramajie, D., De Ojier, J.L.R., Díaz-Losada, E., Díez-Navajas, A.M., Bengoa, P. and Rossi, V. (2019) A Network Meta-Analysis Provides New Insight into Fungicide Scheduling for the Control of *Botrytis cinerea* in Vineyards. *Pest Management Science*, **75**, 324-332. https://doi.org/10.1002/ps.5116

[4] Van Kan, J.A.L., Stassen, J.H.M., Mosbach, A., Van Der Lee, T.A.J., Faino, L., Farmer, A.D., Papasotiriou, D.G., Zhou, S.G., Seidl, M.F., Cottam, E., Edel, D., Hahn, M., Schwartz, D.C., Dietrich, R.A., Widdison, S. and Scalliet, G. (2017) A Gapless Genome Sequence of the Gungus *Botrytis cinerea. Molecular Plant Pathology*, **18**, 75-89. https://doi.org/10.1111/mpp.12384

[5] Nkajima, M. and Akutsu, K. (2014) Virulence Factors of *Botrytis cinerea*. *Journal of General Plant Pathology*, **80**, 15-23. https://doi.org/10.1007/s10327-013-0492-0

[6] González-Fernández, R., Valero-Galván, J., Gómez-Gálvez, F.J. and Jorrin-Novo, J.V. (2015) Unraveling the *in Vitro* Secretome of the Phytopathogen *Botrytis cinerea* to Understand the Interaction with Its Hosts. *Frontiers in Plant Science*, **6**, Article No. 839. https://doi.org/10.3389/fpls.2015.00839

[7] Li, H., Chen, Y., Zhang, Z.Q., Li, B.Q., Qin, G.Z. and Tian, S.P. (2018) Pathogenic Mechanisms and Control Strategies of *Botrytis cinerea* Causing Post-harvest Decay in Fruits and Vegetables. *Food Quality and Safety*, **3**, 111-119. https://doi.org/10.1093/fqsafe/fyy016

[8] Nguyen, T.C., Zaleta-Rivera, K., Huang, X.R., Dai, X.F. and Zhong, S. (2018) RNA, Action through Interactions. *Trends in Genetics*, **34**, 867-882. https://doi.org/10.1016/j.tig.2018.08.001

[9] Qian, X.Y., Zhao, J.Y., Yeung, P.Y., Zhang, Q.F.C. and Kwok, C.K. (2019) Revealing LncRNA Structures and Interactions by Sequencing Based Approaches. *Trends in Genetics*, **44**, 33-52. https://doi.org/10.1016/j.tibs.2018.09.012

[10] Achkar, N.P., Cambiagno, D.A. and Manavella, P.A. (2016) miRNA Biogenesis: A Dynamic Pathway. *Trends in Genetics*, **21**, 1034-1044. https://doi.org/10.1016/j.tplants.2016.09.003

[11] Neumeier, J. and Meister, G. (2021) siRNA Specificity: RNAi Mechanisms and Strategies to Reduce Off-Target Effects. *Frontiers in Plant Science*, **11**, Article ID: 526455. https://doi.org/10.3389/fpls.2020.526455

[12] Langmead, B., Trapnell, C., Pop, M. and Salzberg, S.L. (2009) Ultrafast and Memory-Efficient Alignment of Short DNA Sequences to the Human Genome. *Genome Biology*, **10**, R23. https://doi.org/10.1186/gb-2009-10-3-r25

[13] Nawrocki, E.P. and Eddy, S.R. (2013) Infernal 1.1:100-Fold Faster RNA Homology Searches. *Bioinformatics*, **29**, 2933-2935. https://doi.org/10.1093/bioinformatics/btt509

[14] Friedländer, M.R., Chen, W., Adamidi, C., Maaskola, J., Einspanier, R., Knespel, S. and Rajewsky, N. (2008) Discovering MicroRNAs from Deep Sequencing Data Using MiRDeep. *Nature Biotechnology*, **26**, 407-415. https://doi.org/10.1038/nbt1394

[15] Evers, M., Huttner, M., Dueck, A., Meister, G. and Engelmann, J.C. (2015) MiRA: Adaptable Novel MiRNA Identification in Plants Using Small RNA Sequencing Data. *BMC Bioinformatics*, **16**, Article No. 370. https://doi.org/10.1186/s12859-015-0798-3

[16] Jagla, B., Aulner, N., Kelly, P.D., Song, D., Volchuk, A., Zatorski, A., Shum, D., Mayer, T., De Angelis, D.A., Ouerfelli, O., Rutishauser, U. and Rothman, J.E. (2005) Sequence Characteristics of Functional SiRNAs. *RNA*, **11**, 864-872. https://doi.org/10.1261/rna.7275905

[17] Hoen, P.A.C., Ariyurek, Y., Thygesen, H.H., Vreugdenhil, E., Vossen, R.H.A.M., De Menezes, R.X., Boer, J.M., Van Ommen, G.B. and Den Dunnen, J.T. (2008) Deep Sequencing-Based Expression Analysis Shows Major Advances in Robustness, Resolution and Inter-Lab Portability over Five Microarray Plat Forms. *Nucleic Acids Research*, **36**, e141. https://doi.org/10.1093/nar/gkn705

[18] Bonnet, E., He, Y., Billiau, K. and De Peer, Y.V. (2010) TAPIR, a Web Werver for the Prediction of Plant MicroRNA Targets, Including Target Mimics. *Bioinformatics*, **26**, 1566-1568. https://doi.org/10.1093/bioinformatics/btq233

[19] Yadav, A., Sanyal, I., Rai, S.P. and Lata, C. (2021) An Overview on MiRNA-Encoded Peptides in Plant Biology Research. *Genomics*, **113**, 2385-2391. https://doi.org/10.1016/j.ygeno.2021.05.013

[20] Jonas, S. and Izaurralde, E. (2015) Towards a Molecular Understanding of MicroRNA-Mediated Gene Silencing. *Nature Review Genetics*, **16**, 421-433. https://doi.org/10.1038/nrg3965

[21] Iwakawa, H.O. and Tomari, Y. (2015) The Functions of MicroRNAs: mRNA Decay and Translational Repression. *Trends in Cell Biology*, **25**, 651-665. https://doi.org/10.1016/j.tcb.2015.07.011

[22] Lee, H.C., Li, L.D., GU, W.F., Xue, Z.H., Crosthwaite, S.K., Pertsemlidis, A., Lewis, Z.A., Freitag, M., Selker, E.U., Mello, C.C. and Liu, Y. (2010) Divers Ppathways Generate MicroRNA-Like RNAs and Dicer-Independent Small Interfering RNAs in Fungi. *Molecular Cell*, **38**, 803-814. https://doi.org/10.1016/j.molcel.2010.04.005

[23] Lin, Y.L., Ma L.T., Lee, Y.R., Lin, S.S., Wang, S.Y., Chang, T.T., Shaw, J.F., Li, W.H.

and Chu, F.H. (2015) MicroRNA-Like Small RNAs Prediction in the Development of *Antrodia cinnamomea*. *PLoS ONE*, **10**, e0123245. https://doi.org/10.1371/journal.pone.0123245

[24] Wang, B., Sun, Y.F., Song, N., Zhao, M.X., Liu, R., Feng, H., Wang, X.J. and Kang, Z.S. (2017) *Puccinia striiformis* f. sp. *tritici* MicroRNA-Like RNA 1 (Pst-milR1), an Important Pathogenicity Factor of *Pst*, Impairs Wheat Resistance to *Pst* by Suppressing the Wheat Pathogenesis-Related 2 Gene. *New Phytologist*, **215**, 338-350. https://doi.org/10.1111/nph.14577

[25] Jin, Y., Zhao, J.H., Zhao, P., Zhang, T., Wang, S. and Guo, H.S. (2018) A Fungal MilRNA Mediates Epigenetic Repression of a Virulence Gene in *Verticillium dahlia*. *Philosophical Transactions B of the Royal Society*, **4**, Article ID: 20180309. https://doi.org/10.1098/rstb.2018.0309

[26] Hu, X.Y., Hoden, K.P., Liao, Z., Asman, A. and Dixelius, C. (2022) *Phytophthora infestans* Ago1-Associated MiRNA Promotes Potato Late Blight Disease. *New Phytologist*, **233**, 443-457. https://doi.org/10.1111/nph.17758

[27] Meister, G. and Tuschl, M. (2004) Mechanisms of Gene Silencing by Double-Stranded RNA. *Nature*, **431**, 343-349. https://doi.org/10.1038/nature02873

[28] Jinek, M. and Doudna, J.A. (2009) A Three-Dimensional View of the Molecular Machinery of RNA Interference. *Nature*, **457**, 405-412. https://doi.org/10.1038/nature07755

[29] Meister, G. (2013) Argonaute Proteins: Functional Insights and Emerging Roles. *Nature*, **14**, 864-872. https://doi.org/10.1038/nrg3462

[30] Khatri, M. and Rajam, M.V. (2007) Targeting Polyamines of *Aspergillus nidulans* by SiRNA Specific to Fungal Ornithine Decarboxylase Gene. *Medical Mycology*, **45**, 211-220. https://doi.org/10.1080/13693780601158779

[31] Hammond, T.M., Xiao, H., Boone, E.C., Decker, L.M., Lee, S.A., Perdue, T.D., Pukkila, P.J. and Shiu, P.K.T. (2013) Novel Proteins Required for Meiotic Silencing by Unpaired DNA and SiRNA Generation in *Neurospora crassa*. *Genetics*, **194**, 91-100. https://doi.org/10.1534/genetics.112.148999

[32] Deshmukh, R. and Purohi, H.J. (2014) SiRNA Mediated Gene Silencing in *Fusarium* sp. HKF15 for Overproduction of Bikaverin. *Bioresource Technology*, **157**, 368-371. https://doi.org/10.1016/j.biortech.2014.02.057

[33] Yu, R., Jih, G., Iglesias, N. and Moazed, D. (2014) Determinants of Heterochromatic SiRNA Biogenesis and Function. *Molecular Cell*, **53**, 262-276. https://doi.org/10.1016/j.molcel.2013.11.014

[34] Yu, H., Tsuchida, M., Ando, M., Hashizaki, T., Shimada, A., Takahata, S. and Murakami, Y. (2021) Trimethylguanosine Synthase 1 (TGS1) Is Involved in Swi6/HP1-Independent SiRNA Production and Establishment of Heterochromatin in Fission Yeast. *Genes to Cells*, **26**, 203-218. https://doi.org/10.1111/gtc.12833

Supplemental Material

Table S1. Information of predicted siRNAs in *B. cinerea*.

Name	Guide sequence	Passenger sequence	TPM
Bc-sir1	GGTCGGTCGATTCTAAGTCCC	AGCCAGCTAAGATTCAGGGCC	0.82
Bc-sir2	CGCTATGATACGAGTCCTCCA	TCGCGATACTATGCTCAGGAG	0.50
Bc-sir3	GGCCTATGCTCGAATACATTAGC	GTCCGGATACGAGCTTATGTAAT	0.50
Bc-sir4	AGCGAATCCCCACTGTTGTATG	GGTCGCTTAGGGGTGACAACAT	-
Bc-sir5	ATGTGTTCGAAGTCTAGCCAT	CACAAGCTTCAGATCGGTAGA	-
Bc-sir6	CACAAGCCTCAGATCGGTAGA	ATGTGTTCGGAGTCTAGCCAT	-
Bc-sir7	AAATGGTTCTACCTGGATGCAT	TACCAAGATGGACCTACGTAAT	0.91
Bc-sir8	CTGGGTCCTGAACGTAGT	GCGACCCAGGACTTGCAT	0.82
Bc-sir9	CGCTGGGTCCTGAACGTAGT	CGGCGACCCAGGACTTGCAT	3.41
Bc-sir10	CGCTGGGTCCTGAACGTAGT	TGGCGACCCAGGACTTGCAT	0.55
Bc-sir11	CCGCTGGGTCCTGAACGTAGT	GCGGCGACCCAGGACTTGCAT	2.45
Bc-sir12	GCCGCTGGGTCCTGAACGTAGT	CGCGGCGACCCAGGACTTGCAT	1.36
Bc-sir13	GTCCTGTAAGTAGTAGAGTAGC	GCCAGGACATTCATCATCTCAT	0.50
Bc-sir14	AGCCTTGTTGTTACGATCTACT	CATCGGAACAACAATGCTAGAT	0.50
Bc-sir15	TACTACCGATTGAATGGCTAAG	CGATGATGGCTAACTTACCGAT	0.59
Bc-sir16	GAAGTCGGAATCCGCTAAG	ACCTTCAGCCTTAGGCGAT	0.68
Bc-sir17	AATCGGTTTGTCCGGAGCTAGG	CTTTAGCCAAACAGGCCTCGAT	1.27
Bc-sir18	GTATCTGAGTTATGGTTCGAT	TAGACTCAATACCAAGCTAAG	2.00
Bc-sir19	GTGTTCAAAGCAGGCCTATG	CTCACAAGTTTCGTCCGGAT	0.73
Bc-sir20	TACGACTTAATTGTGCTATACG	GTATGCTGAATTAACACGATAT	0.64
Bc-sir21	TAAGCGCCCTGCATGATATATT	TCATTCGCGGGACGTACTATAT	-
Bc-sir22	ACATAAAGCTAGGAAGGTTTAT	TATTTCGATCCTTCCAAATATA	0.50
Bc-sir23	GTATCGCGAGAGTTAAGAACT	TAGCGCTCTCAATTCTTGATC	15.04
Bc-sir24	AATCGAGTTGCTTGTGGGAGG	CTTTAGCTCAACGAACACCCT	0.45
Bc-sir25	CGATTGCTACAATTCCTCCCT	TAACGATGTTAAGGAGGGAGG	0.86
Bc-sir26	CCGATCTTGATGTCTTCGGATG	CTGGCTAGAACTACAGAAGCCT	1.14
Bc-sir27	CGGCAAGTTACCGGGTCTGCCT	CGTTCAATGGCCCAGACGGAAA	-
Bc-sir28	ATGGAATAATAGAATAGGACG	CGTACCTTATTATCTTATCCT	0.55
Bc-sir29	GGATTCCGATAGTTACACTTCCT	TAAGGCTATCAATGTGAAGGATG	3.27
Bc-sir30	CGCACAAGTAGAGTGATCGAAA	TCGCGTGTTCATCTCACTAGCT	0.45
Bc-sir31	GGTTCTGACGTGCAAATCGATC	CGCCAAGACTGCACGTTTAGCT	0.82
Bc-sir32	GAAGACTAACTACTGCGAAA	AACTTCTGATTGATGACGCT	0.55
Bc-sir33	TCCATTGCACATCGGGGCGACG	GGAGGTAACGTGTAGCCCCGCT	0.77
Bc-sir34	TAGTTACTCGAGTCGGAGGCT	CAATGAGCTCAGCCTCCGATT	0.64
Bc-sir35	ATAGTTACTCGAGTCGGAGGCT	TCAATGAGCTCAGCCTCCGATT	0.50

Continued

Bc-sir36	GCAGCGTTTTGTCTAACCGGCT	TCGCAAAACAGATTGGCCGAAT	2.68
Bc-sir37	AAAACCAGATTGCCCGCAGAGT	GCTTTTGGTCTAACGGGCGTCT	-
Bc-sir38	ATGGAAGAGCCTCGCAAAAGT	CCTTCTCGGAGCGTTTTCAGA	2.32
Bc-sir39	AATGGAAGAGCCTCGCAAAAGT	ACCTTCTCGGAGCGTTTTCAGA	1.32
Bc-sir40	GAATTCGCGGTAGGTAAAAGT	TAAGCGCCATCCATTTTCAGG	0.50
Bc-sir41	GGAGTGCAACCCCTCGGCAAGT	TCACGTTGGGGAGCCGTTCAAT	-
Bc-sir42	CAATGGTCGGTCGATTCTAAGT	TACCAGCCAGCTAAGATTCAGG	0.68
Bc-sir43	TCCTTGGAACAGGACGTCATA	CAAGGAACCTTGTCCTGCAGT	0.68
Bc-sir44	TAAATCGGAGGCTGAGCTCATT	AAATTTAGCCTCCGACTCGAGT	0.86
Bc-sir45	CTATACTTCCCTTACGCATAGT	TATGAAGGGAATGCGTATCAAG	1.91
Bc-sir46	AAATTTAGTTACCCGGGCTAGT	TAAATCAATGGGCCCGATCAGA	-
Bc-sir47	CTATATAACGCGGTAGCGGTAGT	TATATTGCGCCATCGCCATCAAG	1.50
Bc-sir48	TCGCAATTTTTACCCCCATCACT	GTAGCGTTAAAAATGGGGGTAGT	0.55
Bc-sir49	TAACTCCTTCGCTGAAATTTAGT	TGAGGAAGCGACTTTAAATCAAT	-
Bc-sir50	TAATGGCAGGCTCTAAAATCAGT	TCATTACCGTCCGAGATTTTAGT	0.95
Bc-sir51	GTGGGGTTGAATCCTTTGCATA	CGCACCCCAACTTAGGAAACGT	0.91
Bc-sir52	CGTATATTAAAGTTGTTGCAGT	TCGCATATAATTTCAACAACGT	0.55
Bc-sir53	ACTATGCTCAGGAGGTAACGT	ATACGAGTCCTCCATTGCACA	0.82
Bc-sir54	CTCAAAGATTAAGCCATGCATG	CAGAGTTTCTAATTCGGTACGT	0.45
Bc-sir55	CGGATCTCTTGGTTCTGGCATC	TTGCCTAGAGAACCAAGACCGT	0.64
Bc-sir56	TAATAACTTAACGAATCGCATG	GTATTATTGAATTGCTTAGCGT	2.36
Bc-sir57	TCAGGGGGTTCGGCCTAGCATC	AAAGTCCCCCAAGCCGGATCGT	2.41
Bc-sir58	ACTAACTACTGCGAAAGCATT	TCTGATTGATGACGCTTTCGT	0.55
Bc-sir59	GCATTCGACAGCTGCCGCAAGGT	TAAGCTGTCGACGGCGTTCCACC	0.64
Bc-sir60	GCAGGATAAGATAATAAGGT	TCCTATTCTATTATTCCATG	2.23
Bc-sir61	TCGCGATACTATGCTCAGGAGGT	CGCTATGATACGAGTCCTCCATT	0.45
Bc-sir62	TGACTAAAATCTCGGACGGT	TGATTTTAGAGCCTGCCATT	0.45
Bc-sir63	GGACTGAAATTAAATAGCGGT	TGACTTTAATTTATCGCCAGT	3.14
Bc-sir64	TGTCCTGGGTCGCCGCGGCGGT	AGGACCCAGCGGCGCCGCCACT	0.59
Bc-sir65	AGTCCTGGGTCGCCGCGGCGGT	AGGACCCAGCGGCGCCGCCACT	16.41
Bc-sir66	TATCCCTCATCAACCAGCCAAT	GTATAGGGAGTAGTTGGTCGGT	0.59
Bc-sir67	AGATAGTTAACGTCGGAGGGT	TATCAATTGCAGCCTCCCACA	0.45
Bc-sir68	TCTACTGGCACCGAGTACGGGT	ATGACCGTGGCTCATGCCCATG	0.50
Bc-ir69	TATGATGCAAGTCCTGGGT	ACTACGTTCAGGACCCAGC	0.68
Bc-sir70	TTATGATGCAAGTCCTGGGT	TACTACGTTCAGGACCCAGC	2.82
Bc-sir71	CGAAAGACTAATCGAACCATC	CCGCTTTCTGATTAGCTTGGT	0.55
Bc-sir72	GCGAAAGACTAATCGAACCATC	CCCGCTTTCTGATTAGCTTGGT	0.86

Continued

Bc-sir73	CCACTCCGCCTGGCCGGTTGGT	TGAGGCGGACCGGCCAACCAGG	4.86
Bc-sir74	TGATTACTTCAGCGGCTAATGT	TAATGAAGTCGCCGATTACATT	0.73
Bc-sir75	ATGCTCAGGAGGTAACGTGT	CGAGTCCTCCATTGCACATC	1.82
Bc-sir76	CTATGCTCAGGAGGTAACGTGT	TACGAGTCCTCCATTGCACATC	1.32
Bc-sir77	ATCGAATCTTTGAACGCACATT	AGTAGCTTAGAAACTTGCGTGT	0.59
Bc-sir78	GAAGTTTGAGGCAATAACAGG	ACCTTCAAACTCCGTTATTGT	0.73
Bc-sir79	TGATCGGGCCCATTGATTTAAAG	AGACTAGCCCGGGTAACTAAATT	-
Bc-sir80	TCAGCCGTATCAAATACCAATT	TCGGCATAGTTTATGGTTAAGA	2.54
Bc-sir81	TGAGGAAGCACCTTGCGTAATT	GCACTCCTTCGTGGAACGCATT	-
Bc-sir82	TCAGTAATGGCAGGCTCTAAAA	ACAGTCATTACCGTCCGAGATT	2.77
Bc-sir83	GTGGTAATTCTAGAGCTAATA	GGCACCATTAAGATCTCGATT	0.45
Bc-sir84	GTATCTGAGTTATGGTTCGATT	TAGACTCAATACCAAGCTAAGC	0.68
Bc-sir85	TGATTCCAGACTGGCGATAAAT	CGACTAAGGTCTGACCGCTATT	1.14
Bc-sir86	TGGCAAGCCAGATCCCATAATT	TCACCGTTCGGTCTAGGGTATT	0.55
Bc-sir87	GGATGCTCCGGCTTTGGTATT	TACGAGGCCGAAACCATAAGA	0.50
Bc-sir88	ATAGCAGCGTGGTTATGGTTATT	TCGTCGCACCAATACCAATAACT	1.32
Bc-sir89	CGGCGCCGCTGGGTCCTGAACG	CCGCCGCGGCGACCCAGGACTT	0.64
Bc-sir90	TGGCGGATGCCTTCCTGGAATG	GGACCGCCTACGGAAGGACCTT	0.59
Bc-sir91	ACACTAGCCTTAAACCCCCCTT	TGATCGGAATTTGGGGGGAAGT	0.77
Bc-sir92	CCACCTCAACACACTAGCCTT	TGGAGTTGTGTGATCGGAATT	0.50
Bc-sir93	GCAAGTTACCGGGTCTGCCTT	TTCAATGGCCCAGACGGAAAA	-
Bc-sir94	GGATCTTTGGTTGTTTTATCTT	TAGAAACCAACAAAATAGAACC	0.50
Bc-sir95	TCGGGGGCATCAGTATTCAATT	TCAGCCCCCGTAGTCATAAGTT	0.50
Bc-sir96	GAGGGACTATCGGCTCAAGC	ATCTCCCTGATAGCCGAGTT	0.55
Bc-sir97	ATATATAGGATTCCGATAGTT	TATATCCTAAGGCTATCAATG	0.50
Bc-sir98	TATTGCGCCATCGCCATCAAGT	ATATAACGCGGTAGCGGTAGTT	1.41
Bc-sir99	TAGGGTAGGACACGCTGCAATA	CTATCCCATCCTGTGCGACGTT	0.68
Bc-sir100	GGATTACCGGGTTGCATGGGTT	TAATGGCCCAACGTACCCAACC	1.64
Bc-sir101	TTACCGGGTCTGCCTTTTGGTT	TGGCCCAGACGGAAAACCAATA	-
Bc-sir102	GAATGTCCTGGCATATCGTGTT	TACAGGACCGTATAGCACAATT	14.31
Bc-sir103	TGATTCCAGACTGGCGATAAATT	CGACTAAGGTCTGACCGCTATTT	1.14
Bc-sir104	GCAAGTTACCGGGTCTGCCTTT	TTCAATGGCCCAGACGGAAAAC	-
Bc-sir105	TTAAGCCTCCATTGCCCAAATT	AGAATTCGGAGGTAACGGGTTT	0.45
Bc-sir106	TAATGGCAGGCTCTAAAATC	TCATTACCGTCCGAGATTTT	0.68
Bc-sir107	CAAGTTACCGGGTCTGCCTTTT	TCAATGGCCCAGACGGAAAACC	-
Bc-sir108	GCAAGTTACCGGGTCTGCCTTTT	TTCAATGGCCCAGACGGAAAACC	-
Bc-sir109	TGCAATATGTGCTGTCGAAAATG	CGACGTTATACACGACAGCTTTT	0.59
Bc-sir110	TCAGGTGTGAGGCCCCGAAAATC	TCAGTCCACACTCCGGGGCTTTT	1.23

TPM: transcripts per kilobase million; the "-" indicates "not applicable".

Table S2. Target genes prediction of miRNAs in *B. cinerea* using software TAPIR and target finder.

miRNA ID	Target ID	TAPIR Score	TAPIR MFE	Target Finder Score	Pathway	NR ID
miR-1277-5p_2	BCIN_01g00260	4.5	−22.8	3.5	K00102	XP_001545605.1
miR-1277-5p_2	BCIN_01g00440	3	−20.7	3	K00667	XP_018068696.1
miR-1277-5p_2	BCIN_01g00550	2.5	−23.7	3	K07901	XP_001547449.1
miR-1277-5p_2	BCIN_01g00560	2.5	−22.1	-	-	EMR89982.1
miR-1277-5p_2	BCIN_01g00750	5	−20.3	3	K05740	XP_001547248.1
miR-1277-5p_2	BCIN_01g00830	3.5	−26.6	-	K11294	XP_001547258.1
miR-1277-5p_2	BCIN_01g03250	2	−21.1	2	-	XP_001550948.1
miR-1277-5p_2	BCIN_01g04370	3	−24.8	2	K08869	XP_001549015.1
miR-1277-5p_2	BCIN_01g04580	-	NA	3	K11244	CCD55062.1
miR-1277-5p_2	BCIN_01g08210	5	−21.4	2.5	K03260	EMR89818.1
miR-1277-5p_2	BCIN_01g08890	3	−20.5	3	-	CCD45998.1
miR-1277-5p_2	BCIN_01g09710	-	NA	3.5	-	EMR81406.1
miR-1277-5p_2	BCIN_02g01810	3	−22.4	2.5	K05770	XP_001597624.1
miR-1277-5p_2	BCIN_02g01870	5	−21.6	2.5	K05894	XP_001558929.1
miR-1277-5p_2	BCIN_02g02400	3.5	−26.2	3.5	K10958	CCD48604.1
miR-1277-5p_2	BCIN_02g02900	3.5	−23.3	-	K14309	EMR82742.1
miR-1277-5p_2	BCIN_02g05750	-	-	3.5	K03469	XP_001552711.1
miR-1277-5p_2	BCIN_02g07730	-	-	3.5	-	EMR81378.1
miR-1277-5p_2	BCIN_03g01840	2	−21.2	2	K08773	CCD44002.1
miR-1277-5p_2	BCIN_03g03300	-	-	3	K06004	XP_001560517.1
miR-1277-5p_2	BCIN_03g03920	NA	NA	3	-	XP_001560602.1
miR-1277-5p_2	BCIN_03g05330	2	−21.1	2	K06215	CCD51582.1
miR-1277-5p_2	BCIN_03g05820	3.5	−24.2	2	K01728	XP_001560884.1
miR-1277-5p_2	BCIN_03g07100	2	−21.2	2	K11702	CCD51306.1
miR-1277-5p_2	BCIN_03g07560	3	−26.5	3	K11501	EMR83782.1
miR-1277-5p_2	BCIN_03g08670	-	-	3.5	K17808	XP_001554883.1
miR-1277-5p_2	BCIN_04g02270	1	−26.3	1	K18626	XP_001557298.1
miR-1277-5p_2	BCIN_04g05390	3.5	−29.6	-	K14963	XP_001557671.1
miR-1277-5p_2	BCIN_05g00590	1.5	−23	1.5	K21820	XP_001552023.1
miR-1277-5p_2	BCIN_05g00860	5	−21.4	2.5	K01674	XP_001552065.1
miR-1277-5p_2	BCIN_05g02150	3.5	−26.6	-	-	CCD34040.1
miR-1277-5p_2	BCIN_05g02180	3	−26.3	-	-	EMR89408.1
miR-1277-5p_2	BCIN_05g05050	3.5	−21.8	3.5	-	CCD53614.1
miR-1277-5p_2	BCIN_05g06080	3	−25.8	-	-	XP_001559616.1
miR-1277-5p_2	BCIN_05g06090	2.5	−26.1	2.5	-	XP_001559615.1

Continued

miR-1277-5p_2	BCIN_05g06840	2	−23.8	2	K07300	EMR80478.1
miR-1277-5p_2	BCIN_05g08020	1.5	−26.6	1.5	K00088	CCD34394.1
miR-1277-5p_2	BCIN_05g08280	4.5	−20.7	3	K00088	XP_001548411.1
miR-1277-5p_2	BCIN_06g01060	3.5	−19.4	-	K03380	XP_001560250.1
miR-1277-5p_2	BCIN_06g03920	3.5	−26.6	2	K01183	CCD48175.1
miR-1277-5p_2	BCIN_06g05580	-	-	3	-	CCD56961.1
miR-1277-5p_2	BCIN_06g06140	2	−26.3	2	K11681	XP_001549229.1
miR-1277-5p_2	BCIN_06g06150	5	−20.3	3	K20307	XP_001549231.1
miR-1277-5p_2	BCIN_06g07080	2	−21.2	2	K13341	XP_001596816.1
miR-1277-5p_2	BCIN_06g07120	3.5	−21.7	3.5	K00480	EMR90947.1
miR-1277-5p_2	BCIN_06g07250	1.5	−22.8	1.5	-	XP_001545249.1
miR-1277-5p_2	BCIN_07g02120	5	−24.4	3	K09419	CCD46226.1
miR-1277-5p_2	BCIN_07g03250	4	−23.1	3	-	EMR80900.1
miR-1277-5p_2	BCIN_07g07090	1	−24.3	1	-	XP_001549837.1
miR-1277-5p_2	BCIN_08g01170	-	-	2.5	-	XP_001548743.1
miR-1277-5p_2	BCIN_08g01730	-	-	3	K19898	CCD34005.1
miR-1277-5p_2	BCIN_08g02270	-	-	3	-	XP_001551936.1
miR-1277-5p_2	BCIN_08g02590	2	−24.4	2	K19851	XP_001551972.1
miR-1277-5p_2	BCIN_08g02920	-	-	2.5	K07836	APA11004.1
miR-1277-5p_2	BCIN_08g03490	2.5	−22.5	2.5	K20059	XP_001554617.1
miR-1277-5p_2	BCIN_08g03500	2	−21.1	2.5	K15505	XP_001554616.1
miR-1277-5p_2	BCIN_08g03550	2.5	−23.3	NA	K02265	XP_001554609.1
miR-1277-5p_2	BCIN_08g04630	4.5	−22.8	2.5	-	XP_001552328.1
miR-1277-5p_2	BCIN_08g04770	1.5	−22.9	1.5	K02858	XP_001552345.1
miR-1277-5p_2	BCIN_08g04810	3	−20.5	3	K01288	XP_001552353.1
miR-1277-5p_2	BCIN_08g05880	3.5	−23.5	-	-	EMR85246.1
miR-1277-5p_2	BCIN_08g06160	5	−21.5	3.5	K01224	CCD55537.1
miR-1277-5p_2	BCIN_08g06660	3.5	−18.8	-	K11294	EMR85173.1
miR-1277-5p_2	BCIN_09g03880	1	−24.4	1	K16261	XP_001551566.1
miR-1277-5p_2	BCIN_09g05430	-	-	3.5	K02974	EMR83128.1
miR-1277-5p_2	BCIN_09g05440	3.5	−25.5	NA	-	CCD33681.1
miR-1277-5p_2	BCIN_09g06600	-	-	3.5	-	CCD50123.1
miR-1277-5p_2	BCIN_10g00480	-	-	3.5	K01183	ESZ93861.1
miR-1277-5p_2	BCIN_10g00790	3.5	−25.3	NA	K08853	CCD49512.1
miR-1277-5p_2	BCIN_10g01210	2	−21.1	2	-	KIV87681.1
miR-1277-5p_2	BCIN_10g03450	2	−21.1	2	-	CCD49648.1
miR-1277-5p_2	BCIN_10g03890	3	−23.4	3	K00223	XP_001546106.1

Continued

miR-1277-5p_2	BCIN_10g03900	3	−22.6	3.5	-	EMR89744.1
miR-1277-5p_2	BCIN_10g04000	3	−24.1	3	K10733	CCD43707.1
miR-1277-5p_2	BCIN_10g04240	-	-	3.5	-	CCD50947.1
miR-1277-5p_2	BCIN_10g05170	2	−21.2	2	K05747	XP_001546835.1
miR-1277-5p_2	BCIN_11g01410	5	−20.6	2.5	K19898	CCD47615.1
miR-1277-5p_2	BCIN_11g01560	3.5	−19.7	3.5	-	CCD47637.1
miR-1277-5p_2	BCIN_11g02190	-	-	3.5	-	CCD47723.1
miR-1277-5p_2	BCIN_11g02230	3	−22.6	2	K11761	CCD47729.1
miR-1277-5p_2	BCIN_11g02810	3	−20.1	3	-	CCD47816.1
miR-1277-5p_2	BCIN_11g04340	3	−23.7	2	K11680	XP_001558503.1
miR-1277-5p_2	BCIN_11g05350	2	−21.2	2	K11231	EMR87397.1
miR-1277-5p_2	BCIN_12g03700	3	−26.3	3	K03885	PBP26832.1
miR-1277-5p_2	BCIN_12g04550	2	−21.3	2	-	XP_001553933.1
miR-1277-5p_2	BCIN_13g01860	4	−20.1	3	K03448	CCD54498.1
miR-1277-5p_2	BCIN_13g02020	2.5	−26.5	2.5	K01183	ESZ95604.1
miR-1277-5p_2	BCIN_13g02670	1	−28.5	1	K03381	CCD54378.1
miR-1277-5p_2	BCIN_13g03630	2	−21.2	2	K08257	CCD47037.1
miR-1277-5p_2	BCIN_13g04680	3	−24.7	3	-	CCD52364.1
miR-1277-5p_2	BCIN_14g03850	-	-	2.5	K04043	ESZ96837.1
miR-1277-5p_2	BCIN_14g03890	3	−19.6	3	K00898	EMR89147.1
miR-1277-5p_2	BCIN_14g04990	3	−20.4	3	-	XP_001545815.1
miR-1277-5p_2	BCIN_14g05220	1.5	−22.4	1.5	-	CCD43638.1
miR-1277-5p_2	BCIN_15g01340	1.5	−23.5	1.5	K19851	ESZ89649.1
miR-1277-5p_2	BCIN_15g03180	-	-	3.5	-	-
miR-1277-5p_2	BCIN_15g04430	3.5	−19	3.5	K05747	CCD34180.1
miR-1277-5p_2	BCIN_15g04440	-	-	2	K12604	XP_001548505.1
miR-1277-5p_2	BCIN_15g04470	-	-	3.5	K05906	XP_001548502.1
miR-1277-5p_2	BCIN_15g04990	3.5	−21	-	K11314	APA13791.1
miR-1277-5p_2	BCIN_15g05690	2	−21.1	2	K06123	CCD43447.1
miR-1277-5p_2	BCIN_16g04560	3	−21.2	3	K20306	CCD56008.1
miR-4003c-5p	BCIN_04g02950	3.5	−26.7	-	-	EMR88909.1
miR-4003c-5p	BCIN_05g02800	3.5	−26.7	-	K03380	CCD46646.1
miR-4003c-5p	BCIN_05g03030	3.5	−26.2	-	K20178	CCD46610.1
miR-4003c-5p	BCIN_06g01320	3.5	−24.7	-	-	CCD49174.1
miR-4003c-5p	BCIN_10g05790	3	−28.6	4	-	-
miR-466b-2-3p	BCIN_01g00430	3	−36.4	3	-	XP_001547466.1
miR-466b-2-3p	BCIN_01g00560	3	−26.6	3	-	EMR89982.1

Continued

miR-466b-2-3p	BCIN_01g03160	3	−23.8	3	K00101	EMR80850.1
miR-466b-2-3p	BCIN_01g06270	2	−30.3	2	K01613	XP_001561287.1
miR-466b-2-3p	BCIN_02g02180	3.5	−36.4	3.5	-	XP_001558889.1
miR-466b-2-3p	BCIN_02g08160	3	−31.6	4	K16261	ESZ96655.1
miR-466b-2-3p	BCIN_03g01480	3	−30.3	3	K00432	EMR87195.1
miR-466b-2-3p	BCIN_03g07700	5	−30.5	2	K14692	XP_001546498.1
miR-466b-2-3p	BCIN_04g05380	4	−31.3	3	K05747	CCD45013.1
miR-466b-2-3p	BCIN_05g02470	3	−30.3	4	K10273	XP_001560064.1
miR-466b-2-3p	BCIN_05g06080	4	−26.6	3	-	XP_001559616.1
miR-466b-2-3p	BCIN_05g07010	2	−36.3	2	K10798	XP_001548102.1
miR-466b-2-3p	BCIN_06g05240	2	−30.2	3.5	-	CCD56908.1
miR-466b-2-3p	BCIN_07g02120	2	−28.2	-	K09419	CCD46226.1
miR-466b-2-3p	BCIN_07g04210	2.5	−36.4	2.5	-	-
miR-466b-2-3p	BCIN_07g06160	3.5	−36.4	3.5	K08675	CCD55346.1
miR-466b-2-3p	BCIN_07g06450	3.5	−36.3	2.5	K12604	XP_001547736.1
miR-466b-2-3p	BCIN_07g06530	4.5	−31.1	3.5	-	XP_001547727.1
miR-466b-2-3p	BCIN_08g02920	-	-	3.5	K07836	APA11004.1
miR-466b-2-3p	BCIN_08g05880	-	-	3	-	EMR85246.1
miR-466b-2-3p	BCIN_09g05170	4.5	−35.7	3.5	K01046	XP_001551716.1
miR-466b-2-3p	BCIN_10g01690	3.5	−36.4	3.5	K01183	EMR81038.1
miR-466b-2-3p	BCIN_10g02860	2.5	−35.6	2.5	K11294	XP_001556948.1
miR-466b-2-3p	BCIN_10g03010	2.5	−36.4	1.5	-	XP_001556928.1
miR-466b-2-3p	BCIN_10g03210	2.5	−36.2	2.5	K14213	XP_001548054.1
miR-466b-2-3p	BCIN_10g04260	3.5	−36.3	3.5	-	EMR82279.1
miR-466b-2-3p	BCIN_10g04530	4	−26.4	3	K11294	XP_001557411.1
miR-466b-2-3p	BCIN_10g05100	3	−30.4	3	K01183	EMR81430.1
miR-466b-2-3p	BCIN_12g01280	2	−36.3	2	K20521	CCD53768.1
miR-466b-2-3p	BCIN_12g03680	2	−28.2	2.5	K01183	XP_001552242.1
miR-466b-2-3p	BCIN_13g03710	3.5	−30.8	3.5	K01537	CCD47027.1
miR-466b-2-3p	BCIN_13g04920	4.5	−36	3.5	K11173	ESZ95094.1
miR-466b-2-3p	BCIN_14g00530	3	−27.4	4	-	XP_001547926.1
miR-466b-2-3p	BCIN_15g04120	-	-	3.5	K20042	EMR82018.1
miR-466b-2-3p	BCIN_15g04440	3.5	−36.4	1.5	K12604	XP_001548505.1
miR-466b-2-3p	BCIN_15g04460	4	−26.6	3	K05747	CCD34183.1
miR-466b-2-3p	BCIN_15g04990	3	−27.4	3	K11314	APA13791.1
miR-466b-2-3p	BCIN_16g00770	3.5	−36.4	3	K21293	CCD35042.1
miR-466i-5p	BCIN_01g00430	1	−38.1	1	-	XP_001547466.1

Continued

miR-466i-5p	BCIN_01g00550	3	−34.2	3	K07901	XP_001547449.1
miR-466i-5p	BCIN_01g00920	3.5	−32.9	3.5	-	XP_001555522.1
miR-466i-5p	BCIN_01g00950	5	−32.8	0	K09885	XP_001555528.1
miR-466i-5p	BCIN_01g01790	2.5	−36.2	2.5	K00102	EMR89872.1
miR-466i-5p	BCIN_01g02580	3	−37.1	3	K06630	APA06607.1
miR-466i-5p	BCIN_01g02740	0	−41.9	0	-	EMR81600.1
miR-466i-5p	BCIN_01g03480	3	−33.2	-	K05857	CCD54920.1
miR-466i-5p	BCIN_01g03660	0	−41.8	0	K08773	XP_001551000.1
miR-466i-5p	BCIN_01g04580	5	−27.8	0	K11244	CCD55062.1
miR-466i-5p	BCIN_01g05040	1.5	−38.1	1.5	-	EMR86089.1
miR-466i-5p	BCIN_01g05350	3.5	−34.1	3.5	-	ESZ99262.1
miR-466i-5p	BCIN_01g06010	1	−41.1	1	K11244	APA06865.1
miR-466i-5p	BCIN_01g06260	0.5	−41.5	0.5	K19691	AAL30826.1
miR-466i-5p	BCIN_01g06420	3	−34.8	3	K12488	ESZ98859.1
miR-466i-5p	BCIN_01g06740	3.5	−34.1	1.5	-	XP_001561229.1
miR-466i-5p	BCIN_01g07410	-	-	2.5	-	XP_001561128.1
miR-466i-5p	BCIN_01g07600	3.5	−32.6	3.5	-	XP_001561105.1
miR-466i-5p	BCIN_01g07870	2	−38.1	2	K22193	CCD45851.1
miR-466i-5p	BCIN_01g09100	5	−30	0	K16055	XP_001586238.1
miR-466i-5p	BCIN_01g10630	0.5	−39.8	0.5	-	CCD43118.1
miR-466i-5p	BCIN_02g01080	4.5	−35.4	3.5	K03282	XP_001597483.1
miR-466i-5p	BCIN_02g01870	3.5	−33.9	3.5	K05894	XP_001558929.1
miR-466i-5p	BCIN_02g02310	3	−35	3	K17262	XP_001558870.1
miR-466i-5p	BCIN_02g02410	3	−33.3	2.5	K01183	PBP23908.1
miR-466i-5p	BCIN_02g03320	4.5	−32.9	2	K08064	EMR82704.1
miR-466i-5p	BCIN_02g03490	2	−38.3	2	K01758	KIM97697.1
miR-466i-5p	BCIN_02g04210	3	−35.8	3	-	XP_001553733.1
miR-466i-5p	BCIN_02g04230	1.5	−38.1	1.5	K01183	EMR87251.1
miR-466i-5p	BCIN_02g05030	1.5	−41.1	1.5	K21631	XP_001546736.1
miR-466i-5p	BCIN_02g05460	5	−32.8	3	K21632	EMR82905.1
miR-466i-5p	BCIN_02g05590	3	−33	-	K14568	EMR82918.1
miR-466i-5p	BCIN_02g07390	1	−40	1	K01183	EMR81569.1
miR-466i-5p	BCIN_03g00940	1	−40	1	K11294	XP_001559444.1
miR-466i-5p	BCIN_03g01710	4	−31.7	3	K19851	CCD43982.1
miR-466i-5p	BCIN_03g01790	3	−35.3	3	K03260	XP_001559323.1
miR-466i-5p	BCIN_03g02860	2	−38	2	K09510	XP_001555002.1
miR-466i-5p	BCIN_03g03450	3	−35	-	K12274	CCD51846.1

Continued

miR-466i-5p	BCIN_03g03920	0	−42.1	0	-	XP_001560602.1
miR-466i-5p	BCIN_03g05330	2	−37.2	1.5	K06215	CCD51582.1
miR-466i-5p	BCIN_03g06450	2.5	−36.4	2.5	K20100	CCD51406.1
miR-466i-5p	BCIN_03g07700	3	−35.9	3	K14692	XP_001546498.1
miR-466i-5p	BCIN_03g08150	3.5	−34.6	3	-	EMR81292.1
miR-466i-5p	BCIN_03g08390	0	−42.1	0	-	XP_001554920.1
miR-466i-5p	BCIN_03g08670	5	−31.1	2	K17808	XP_001554883.1
miR-466i-5p	BCIN_03g08840	3.5	−33.1	3.5	K13289	XP_001554862.1
miR-466i-5p	BCIN_04g00220	4	−36.4	3.5	K20301	CCD34150.1
miR-466i-5p	BCIN_04g01650	3.5	−31	3	K11215	CCD46887.1
miR-466i-5p	BCIN_04g02120	1.5	−40.4	1.5	K18045	XP_001557315.1
miR-466i-5p	BCIN_04g03510	3	−32.8	-	K01183	XP_001546962.1
miR-466i-5p	BCIN_04g05140	1.5	−38.1	1.5	-	EMR86951.1
miR-466i-5p	BCIN_04g06150	3	−34.9	3	K08257	XP_001557784.1
miR-466i-5p	BCIN_05g00480	2	−37.7	2	K00759	XP_001550336.1
miR-466i-5p	BCIN_05g01210	3.5	−36.2	2.5	K08257	A0A0B5L7R4.1
miR-466i-5p	BCIN_05g01350	2	−38.3	2	K03141	XP_001549029.1
miR-466i-5p	BCIN_05g01560	1	−38.7	1	K17550	CCD33804.1
miR-466i-5p	BCIN_05g01760	3	−32.7	-	-	XP_001548220.1
miR-466i-5p	BCIN_05g02760	4	−34.8	3.5	K03316	XP_001560021.1
miR-466i-5p	BCIN_05g03070	-	-	2.5	-	XP_001559970.1
miR-466i-5p	BCIN_05g04230	2.5	−37	2	K12198	XP_001559801.1
miR-466i-5p	BCIN_05g06680	3	−36.5	2	K13120	XP_001559538.1
miR-466i-5p	BCIN_05g06880	4	−31.1	2.5	K08286	XP_001548082.1
miR-466i-5p	BCIN_05g07180	-	-	3	K01539	XP_001548124.1
miR-466i-5p	BCIN_05g07560	4	−32.8	3	-	XP_001552695.1
miR-466i-5p	BCIN_05g07590	1	−41.7	1	K00108	XP_001550662.1
miR-466i-5p	BCIN_06g00370	3.5	−33.5	-	K01749	XP_001560154.1
miR-466i-5p	BCIN_06g02840	-	-	3.5	-	XP_001560498.1
miR-466i-5p	BCIN_06g02870	3	−36	3	K14758	EMR88544.1
miR-466i-5p	BCIN_06g02920	2	−36	2	K10689	XP_001556264.1
miR-466i-5p	BCIN_06g03910	3	−36.8	3.5	K20523	XP_001556115.1
miR-466i-5p	BCIN_06g03970	1	−40	1	K07297	EMR86394.1
miR-466i-5p	BCIN_06g04320	2.5	−36.2	2.5	-	CCD56774.1
miR-466i-5p	BCIN_06g05000	1.5	−38.3	1.5	K11552	EMR87611.1
miR-466i-5p	BCIN_06g05800	1.5	−39.8	2	K21543	CCD56999.1
miR-466i-5p	BCIN_06g05940	4.5	−33.5	3	K19475	CCD57022.1

Continued

miR-466i-5p	BCIN_06g06360	4	−31.4	0	K11380	XP_001549253.1
miR-466i-5p	BCIN_06g06500	-	-	2.5	K09584	XP_001555206.1
miR-466i-5p	BCIN_06g07290	3	−35.1	3	-	XP_001547338.1
miR-466i-5p	BCIN_07g00760	3	−33.4	3.5	K01183	XP_001556067.1
miR-466i-5p	BCIN_07g01110	2	−36.5	2	K20872	XP_001551517.1
miR-466i-5p	BCIN_07g01410	3.5	−29.9	3.5	-	EMR91000.1
miR-466i-5p	BCIN_07g01650	-	-	3	-	EMR88033.1
miR-466i-5p	BCIN_07g03500	3	−35.1	3	-	CCD53038.1
miR-466i-5p	BCIN_07g03890	0	−41.9	0	K11294	CCD52989.1
miR-466i-5p	BCIN_07g04210	4	−33	3	-	-
miR-466i-5p	BCIN_07g04420	0	−41.9	0	K19851	XP_001589337.1
miR-466i-5p	BCIN_07g04430	5	−27.8	3	K19838	EMR81973.1
miR-466i-5p	BCIN_07g04660	5	−27.7	3	K11872	CCD52867.1
miR-466i-5p	BCIN_07g04720	4	−33	1	K10688	XP_001554092.1
miR-466i-5p	BCIN_07g06500	3	−36.4	3	-	EMR91055.1
miR-466i-5p	BCIN_07g06960	2	−37.8	2	K11262	XP_001592109.1
miR-466i-5p	BCIN_08g00550	3	−36.2	3	K01120	XP_001552552.1
miR-466i-5p	BCIN_08g01040	1.5	−38.5	1.5	K12879	CCD43777.1
miR-466i-5p	BCIN_08g01620	3	−33	-	K19848	KGY15063.1
miR-466i-5p	BCIN_08g02810	3	−32.4	3	K16216	XP_001551998.1
miR-466i-5p	BCIN_08g02920	3	−36.2	3	K07836	APA11004.1
miR-466i-5p	BCIN_08g03300	1	−40	1	-	CCD54028.1
miR-466i-5p	BCIN_08g03490	3	−33.2	0	K20059	XP_001554617.1
miR-466i-5p	BCIN_08g03550	1	−41.4	1	K02265	XP_001554609.1
miR-466i-5p	BCIN_08g04300	2	−40.7	2.5	K03099	CCD51965.1
miR-466i-5p	BCIN_08g05150	4.5	−27	2.5	K11246	EMR85582.1
miR-466i-5p	BCIN_08g05880	0	−42.1	0	-	EMR85246.1
miR-466i-5p	BCIN_08g06660	3.5	−33	-	K11294	EMR85173.1
miR-466i-5p	BCIN_09g00920	5	−25.7	2.5	K09051	EMR83531.1
miR-466i-5p	BCIN_09g01230	3	−34.9	3	K01115	CCD55073.1
miR-466i-5p	BCIN_09g02560	3	−34.8	3	K20520	CCD44478.1
miR-466i-5p	BCIN_09g03930	4.5	−30.1	3.5	K14171	XP_001551558.1
miR-466i-5p	BCIN_09g04170	2	−36.7	2.5	K00844	EMR80470.1
miR-466i-5p	BCIN_09g04550	1.5	−38.6	1.5	K03114	EMR90311.1
miR-466i-5p	BCIN_09g04580	3.5	−31.1	3	K14692	XP_001593574.1
miR-466i-5p	BCIN_09g04680	4	−33	2.5	K05747	EMR90324.1
miR-466i-5p	BCIN_09g06110	0	−42.1	0	K01638	CZT05650.1

Continued

miR-466i-5p	BCIN_09g06400	-	-	3.5	K21421	CCD50097.1
miR-466i-5p	BCIN_10g00500	-	-	2.5	-	XP_001554208.1
miR-466i-5p	BCIN_10g00940	3	−36.2	3.5	-	CCD49535.1
miR-466i-5p	BCIN_10g01220	0	−41.8	4	K03360	XP_001555738.1
miR-466i-5p	BCIN_10g01230	2.5	−36	2.5	K03006	XP_001555736.1
miR-466i-5p	BCIN_10g01600	3.5	−36.2	3.5	K01469	XP_001555688.1
miR-466i-5p	BCIN_10g02300	2.5	−36.8	3.5	K11397	XP_001557022.1
miR-466i-5p	BCIN_10g02590	3	−34.2	3	K16186	EMR82676.1
miR-466i-5p	BCIN_10g03080	2.5	−34.8	2	K00306	CCD44963.1
miR-466i-5p	BCIN_10g03170	3	−38.3	-	K10669	XP_001548061.1
miR-466i-5p	BCIN_10g03190	4.5	−34.1	3.5	K11240	XP_001548056.1
miR-466i-5p	BCIN_10g03450	4	−31.3	1	-	CCD49648.1
miR-466i-5p	BCIN_10g04090	1	−38.1	1	K01210	CCD43696.1
miR-466i-5p	BCIN_10g04630	2.5	−36.4	3	K00002	XP_001557399.1
miR-466i-5p	BCIN_10g04640	3.5	−34.6	3	K01183	CCD51011.1
miR-466i-5p	BCIN_10g05690	4.5	−30.3	1.5	-	CCD50870.1
miR-466i-5p	BCIN_10g05760	3	−32.9	-	K01183	XP_001551433.1
miR-466i-5p	BCIN_10g05970	3.5	−34	3	K03260	CCD34756.1
miR-466i-5p	BCIN_10g06070	1	−41.3	1	K20523	XP_001545980.1
miR-466i-5p	BCIN_10g06080	3.5	−35.6	-	K05857	CCD34776.1
miR-466i-5p	BCIN_11g00690	1.5	−40.7	1.5	-	CCD34074.1
miR-466i-5p	BCIN_11g00730	2	−38.1	2	-	CCD49456.1
miR-466i-5p	BCIN_11g02230	4.5	−28.8	2	K11761	CCD47729.1
miR-466i-5p	BCIN_11g02410	3.5	−35	-	K21989	EMR89730.1
miR-466i-5p	BCIN_11g03290	2.5	−37.7	2.5	K21543	XP_001556845.1
miR-466i-5p	BCIN_11g04340	1	−41.4	0.5	K11680	XP_001558503.1
miR-466i-5p	BCIN_11g05770	3.5	−36.1	3.5	K03321	EMR90820.1
miR-466i-5p	BCIN_11g05820	2.5	−32.2	2.5	-	CCD50386.1
miR-466i-5p	BCIN_11g06110	3	−34.4	-	K19800	EMR84088.1
miR-466i-5p	BCIN_12g00490	3.5	−34.5	3.5	K01183	CCD45324.1
miR-466i-5p	BCIN_12g00740	3.5	−33	-	K17652	XP_001557920.1
miR-466i-5p	BCIN_12g01240	4	−36.8	2	-	XP_001557861.1
miR-466i-5p	BCIN_12g01830	3.5	−32.8	-	K00953	XP_001550264.1
miR-466i-5p	BCIN_12g01870	3.5	−30.8	3.5	K00344	XP_001550258.1
miR-466i-5p	BCIN_12g02110	2.5	−34.9	3	-	XP_001558052.1
miR-466i-5p	BCIN_12g03180	0	−41.9	0	K00327	CZR63224.1
miR-466i-5p	BCIN_12g03620	1	−37.1	2	K00915	XP_001552249.1

Continued

miR-466i-5p	BCIN_12g03630	3	−37.7	3	-	CCD52608.1
miR-466i-5p	BCIN_12g04510	1.5	−38.7	4	K11231	CCD52712.1
miR-466i-5p	BCIN_13g00890	3.5	−37.4	4	K11254	CEF85879.1
miR-466i-5p	BCIN_13g01840	2.5	−36.2	2.5	K12734	CCD54500.1
miR-466i-5p	BCIN_13g02670	3.5	−32.8	3.5	K03381	CCD54378.1
miR-466i-5p	BCIN_13g04520	2.5	−40.6	2.5	K08052	APA15577.1
miR-466i-5p	BCIN_13g05060	3.5	−34.3	3.5	-	XP_001554822.1
miR-466i-5p	BCIN_14g01000	3	−34.2	3.5	-	XP_001550102.1
miR-466i-5p	BCIN_14g02450	3.5	−33	-	K18338	XP_001553175.1
miR-466i-5p	BCIN_14g03390	3	−35.3	3	K01915	XP_001549470.1
miR-466i-5p	BCIN_14g03860	3	−34.6	4	K12765	CCD50088.1
miR-466i-5p	BCIN_14g04700	4	−28.4	1	K07766	XP_001546171.1
miR-466i-5p	BCIN_14g05050	0	−41.8	0	K03510	CCD43659.1
miR-466i-5p	BCIN_15g00300	3.5	−35.4	3.5	-	XP_001548800.1
miR-466i-5p	BCIN_15g00970	2.5	−34.9	2.5	K11273	EMR89121.1
miR-466i-5p	BCIN_15g01330	5	−35.7	3	K19806	CCD47474.1
miR-466i-5p	BCIN_15g02150	3.5	−34.9	3	K19691	AAR30107.1
miR-466i-5p	BCIN_15g02270	3	−29.7	-	K00693	OWP03119.1
miR-466i-5p	BCIN_15g02310	4.5	−31.1	1	-	XP_001549572.1
miR-466i-5p	BCIN_15g02590	1.5	−37.8	1.5	K01768	CCD47303.1
miR-466i-5p	BCIN_15g05360	4.5	−32.6	2.5	K00965	CCD43388.1
miR-466i-5p	BCIN_16g00370	2.5	−36.3	2.5	K04705	CCD49400.1
miR-466i-5p	BCIN_16g01160	2	−38.5	1.5	K17781	XP_001545267.1
miR-466i-5p	BCIN_16g01560	1	−37.4	1	K07238	EMR81335.1
miR-466i-5p	BCIN_16g02440	4	−31.2	2	K00111	CCD48688.1
miR-466i-5p	BCIN_16g02880	3	−34.3	3	K11877	XP_001551858.1
miR-466i-5p	BCIN_16g04000	0.5	−40	0.5	K18748	APA15448.1
miR-466i-5p	BCIN_16g04330	5	−27.7	3.5	K03083	CCD55978.1
miR-466i-5p	BCIN_16g04910	3	−34.3	0	K11238	EMR80965.1
novel_mir5	BCIN_09g00390	2	−43.1	2	-	XP_001552636.1
novel_mir5	BCIN_14g00350	0	−49.3	0	K21440	EMR91141.1

The "-" indicates "not applicable"; MFE: minimum free energy; NR: non-redundant database.